HHS Public Access

Author manuscript

Appl Mater Today. Author manuscript; available in PMC 2020 August 08.

Published in final edited form as:

Appl Mater Today. 2020 March ; 18: . doi:10.1016/j.apmt.2019.100479.

Hydrogel-based 3D bioprinting: A comprehensive review on cell-laden hydrogels, bioink formulations, and future perspectives

Janitha M. Unagolla[a], **Ambalangodage C. Jayasuriya**[a,b,*]

[a]Biomedical Engineering Program, Department of Bioengineering, College of Engineering, University of Toledo, Toledo, OH 43607, USA

[b]Department of Orthopedic Surgery, College of Medicine and Life Sciences, University of Toledo, Toledo, OH 43614, USA

Abstract

Hydrogel plays a vital role in cell-laden three dimensional (3D) bioprinting, whereas those hydrogels mimic the physical and biochemical characteristics of native extracellular matrix (ECM). The complex microenvironment of the ECM does not replicate from the traditional static microenvironment of the hydrogel, but the evolution of the 3D bioprinting facilitates to accommodate the dynamic modulation and spatial heterogeneity of the hydrogel system. Selection of hydrogel for 3D bioprinting depends on the printing techniques including microextrusion, inkjet, laser-assisted printing, and stereolithography. In this review, we specifically cover the 3D printable hydrogels where cells can be encapsulated without significant reduction in the cell viability. The recent research highlights of the most widely used hydrogel materials are elucidated in terms of stability of the hydrogel system, cross-linking method, support cell types and their post-printing cell viability. Also, the techniques used to improve the mechanical and biological properties of the hydrogels, such as adding various organic and inorganic materials and making microchannels, are discussed. Furthermore, the recent advances in vascularized tissue construct and scaffold-free bioprinting as a promising method for vascularization are covered in this review. The recent trends in four-dimensional (4D) bioprinting as a stimuli-responsive formation of new organs, and 3D bioprinting based organ-on-chip systems are also discussed.

Keywords

Hydrogel; Bioprinting; Microextrusion; Dynamic modulation; Vascularization

1. Introduction

Tissue engineering is one of the promising technique to alleviate the organ shortage crisis in the world by developing artificial tissue and organs [1]. In general, tissue engineering utilizes three elements to generate functional tissue construct: (i) cells alone, (ii)

*Corresponding author at: Department of Orthopaedic Surgery, University of Toledo Medical Center, 3000 Arlington Avenue, Toledo, OH 43614, USA. a.jayasuriya@utoledo.edu (A.C. Jayasuriya).

Declaration of Competing Interest

The authors declare no conflict of interest.

biomaterials alone, and (iii) combination of both cells and materials in the form of scaffolds [2]. The conventional scaffold fabrication techniques, such as solvent casting, gas forming, membrane lamination, salt leaching, and fiber binding [3–5] have limitations including intrinsic inability to mimic the complex microstructure of biological tissues [6]. As a solution to this problem, another tissue engineering approach called modular tissue engineering was investigated to mimic the complex microstructural features of the organ [7,8] before the development of 3D bioprinting techniques. Furthermore, 3D bioprinting based on three approaches: biomimicry, autonomous self-assembly, and mini-tissue building blocks [9]; offers the unprecedented capability and versatility to deliver cells and materials in complex microstructure with superior spatial distribution [10]. So, researches are developing the 3D bioprinting techniques to fabricate 3D human organs with similar biological and mechanical properties to the actual organs. Also, 3D bioprinting allows us to design and produce structures intraoperatively, especially for bone injuries and defects where imaging based bioprinting with the assist of magnetic resonance imaging (MRI) or computed tomography (CT) can be utilized to print scaffolds/grafts that can precisely fit into bone defects [11].

Bioprinting is defined as the spatial patterning of living cells and other biologies such as growth factors by stacking and assembling them using a computer-aided layer by layer deposition technique for fabrication of living tissue and organs [12,13]. However, 3D printing of bioinert materials without biological component cannot be considered as bioprinting [12]. Four types of techniques widely used for the bioprinting, namely, (i) extrusion-based, (ii) inkjetbased, (iii) laser-assisted, and (iv) stereolithography [1,11,17,24]. Inkjet bioprinters are also known as a drop on demand bioprinters. Recently, this drop on demand bioprinters further classified into four groups according to their droplet generation mechanisms, namely inkjet (thermal, piezoelectric or electrostatic) bioprinters, acoustic droplet election, electro-hydrodynamic jetting, and micro-valve bioprinting [21]. In-depth details of these three techniques were extensively studied or reviewed by many researchers [1,12,17,21,24–26], and therefore, we are not going to discuss the details on these techniques in this review paper. The summarized details of each bioprinter type and their basic features are shown in Table 1. The conventional 3D printing involves the printing of synthetic or natural polymer or combination of both using extreme conditions such as heating, prolonged chemical crosslinking, and photocrosslinking. The most used polymers in the 3D printing techniques are the followings: poly(ε-caprolactone) (PCL) [27–29]. poly(lactic acid) (PLA) [30–33], poly(lactic-co-glycolic acid) (PLGA) [34–36], hydrogel-based polymers such as alginate, gelatin, and poly(ethylene glycol) (PEG) based materials (will be discussed in the section 3). Incorporation of inorganic substances such as hydroxyapatite (HA) [37], graphene oxide (GO) [38], β-tricalcium phosphate (β-TCP) [39], and calcium phosphate [30] into thermoplastic polymers was also investigated as a method to improve hydrophilicity and bioactivity.

Many review papers addressed the 3D printing technologies and materials used as a bioink, including thermosets, hydrogels, and inorganic nanocomposites. However, those reviews mostly focused on the printability and cytotoxicity of the materials, and there is a shortage of comprehensive reviews on cell encapsulated hydrogel systems. There are a lot of essential requirements which have to be addressed when we select a hydrogel-based material for cell

encapsulated printng (bioprinting). Therefore, In this review paper, we will discuss the natural and synthetic material systems, which can be used for bioprinting with cells. This paper also reviews the hydrogel structure, stability, and their properties, including, shear-thinning, self-healing, and encapsulated cell viability. The sections are categorized according to the type of hydrogel material such as aliginate, gelatin, and PEG, where the limitations and strength of each bioink materials are elucidated, and different printing techniques are elaborated accordingly. The type of cells and their viability after printing will be discussed with the addition of specific applications. Also, the recent trends in bioprinting such as scaffold-free bioprinting 4D bioprinting, and bioprinting of organ-on-chip systems will be discussed with a focus on the materials perspective rather than the cells. Finally, this paper provides the reader with current and future perspective of bioprintable materials and their limitations.

2. Hydrogel structure, stability, and properties

Hydrogels, a 3D network of molecules composed of hydrophilic polymer chains, can be designed into any shape, size or form, and have the ability to absorb up to a thousand times their dry weight in a water-rich environment [40,41]. Hydrogel-based systems have become a prime candidate for many applications as carriers for cells in various tissue engineering applications, and as molecule or drug delivery vehicles in stem cell and cancer research due to the recent advances in 3D bioprinting techniques [42]. More controlled physicochemical properties of hydrogels have been achieved in the past couple of years due to the advances in chemical methods- such as click chemistry, gelation mechanisms, and mixing with nanoparticles. However, the biomedical engineering related applications, such as tissue engineering, stem cell therapy for cancers, and immunomodulation; require more than mechanical and chemical versatility from hydrogels, require cell compatibility and mimicking the ECM environment for cellular activities. The traditional static and normal microenvironment of hydrogels do not replicate the complexity of the biological tissues since most of the biological processes are heterogeneous in nature. Therefore, a variety of innovative fabrication techniques were evolved not only to cater the dynamic modulation of hydrogels, which attributed to the changing their shapes gradually in the predefined path; but also to control spatial heterogeneity, which determines the tissue integration, localized cell behavior, and cell-material interactions [40–43].

Hydrogels are formed by cross-linking of polymer chains in an aqueous medium through various mechanisms such as physical entanglement, ionic interaction, chemical crosslinking. Physical entanglement or physical gelation mostly depends on the intrinsic properties of the polymers and therefore, the ability to control the microenvironment is limited. However, these gelation processes do not require the complex chemical modification to the chains, and also these processes are generally reversible. In contrast to the physical approach, chemical approach always requires controlled process conditions, but this controllable and precise crosslinking procedures are beneficial to develop more accurate and hierarchically complex microenvironment.

2.1. Physical crosslinking

2.1.1. Thermal condensation—Most of the seaweed-derived natural polysaccharides, including agarose, carrageenan, and some animal-derived protein, including gelatin, elastin, and collagen, make the thermally driven hydrogels [44]. Thermal condensation or gelation (Fig. 1(a)) occurs at either increasing temperature or decreasing temperature, in which the transition temperatures are defined as the upper critical solution temperature (UCST), where above this temperature water and polymer are miscible; and lower critical solution temperature (LCST), where below this temperature water and polymer are miscible [41,44,45]. Three types of possible interactions are taken place when a polymer is dissolved in water, namely polymer-polymer, polymer-water, and water-water [46]. For polymer exhibiting an LCST, temperature increase makes polymer-water interaction unfavorable, making the other two interactions more favorable, which results in negative free energy (ΔG). This negative free energy is attributed to the higher entropy term (ΔS) with respect to the increase in the enthalpy term (ΔH) according to the thermodynamic relation $\Delta G = \Delta H - T\Delta S$. In this type of system, water-water interaction is the governing force and hence the entropy of water is increased. This phenomenon is known as the “hydrophobic effect". It is noteworthy to mention that LCST is an “entropy driven" effect while UCST is an “enthalpy driven" effect [44–46]. Compared to the LCST driven polymers, very few UCST driven polymers have been found to date [47].

2.1.2. Self-assembly—Molecular self-assembly is the other form of physical gelation process. Self-assembly is driven by the noncovalent, weak bonding mechanisms such as hydrogen bonds, hydrophobic interactions, electrostatic interactions, and it is mainly dominated by the peptide and protein-based hydrogels (Fig. 1(b)) [48]. Recent advances in supramolecular chemistry have opened the door for development of an increasing number of bioinspired hydrogel systems. These systems have two distinct properties which are essential for 3D printed hydrogels and injectable gels; they are shear thinning, show viscous flow under shear stress and self-healing, ability to recover when the stress is removed. However, the major challenge in this type of system is the prolonged time for self-healing, which adversely affects the cell encapsulation. Despite these drawbacks, several biomimetic supramolecular systems have been developed utilizing host-guest or receptor-ligand pairs, and dock-and-lock protein structures [49,50].

2.1.3. Ionic interaction—The hydrogel can also be formed either chelation (Fig. 1(c)) or electrostatic interaction (Fig. 1(d)), facilitating spontaneous physical gelation due to the presence of electrically charged species. These polymers are known as polyelectrolytes: contain net charged along the polymer backbone, and crosslink to form insoluble complexes when combined with multi-valent cations or anions according to the charge of the polymer. The reason for the insolubility of these polyelectrolyte complexes in the water is the scarcity of the charged groups of the polymer, which are mutually shielded by the complex formation [44]. This types of physical hydrogels are also known as ionotropic hydrogels [51]. Most of the natural polymers are negatively charged, such as alginate, carrageenan, and hyaluronic acid due to the presence of carboxyl or sulfate groups. However, the presence of the amino groups in the polymer backbone make positively charged polymers like chitosan and gelatin. Calcium alginate is a prominent example for ionotropic hydrogel. Alginate is composed of

α-L-guluronic acid (G units) and β-D-mannuronic acid (M units) monomers, which vary in amount and depending on the source of alginate [52,53]. The presence of divalent cations such as Ca^{2+} and Ba^{2+} facilitate binding between the G-units of the adjacent alginate chains in an “egg-box" form. In contrast to the natural polymers, polyelectrolytes from synthetic polymers offer a wide range of controllable electrostatic properties. The most common example for the synthetic ionotropic hydrogel is the poly (L-lysine) (PLL) and poly (acrylic acid) (PAA) pair [6,54].

2.2. Chemical crosslinking

The most stable and tunable hydrogels can be obtained through the chemical cross-linking (covalently bound hydrogels) (Fig. 1(e)) as compared to the physical cross-linking. Conventional crosslinking mechanisms include radical polymerization, crosslinking through complementary groups such as aldehydes, condensation reactions between hydroxyl or amine groups with carboxylic acids or derivatives, high energy irradiation, and enzyme-enabled crosslinking [55]. Recent developments in the click chemistry provide extremely selective and orthogonal reactions that proceed with high efficiency and under a variety of mild conditions, which enables the biological functionalities within the hydrogel during processing. Furthermore, these advances facilitate well-defined microenvironment for assaying cell functions where single cues can be introduced, and subsequent effects individually elucidated [56,57]. Click chemistry based reactions have been widely used for hydrogel formation in recent years due to the challenges associated with the conventional chemical crosslinking methods such as extreme reaction conditions, prolonged reaction time, and low yield, which adversely affect to the use of cells with the material [41]. Apart from click chemistry, in the past decade, Michael addition has been widely exploited as a bioorthogonal reaction tool, including thiol-based vinyl sulfones, acrylamides, and maleimides. Also, the azide-alkyne cycloaddition reaction was studied as an appropriate cellular encapsulation system [58]. Thiolene reactions are radically mediated polymerization, which requires the creation of initial radicals either thermally or photochemically. Despite, photochemically driven radical formation provides additional benefits to fabricate cell encapsulated matrices: (i) the ability to spatiotemporally control the chemistry, (ii) rapid reaction rate at a lower radical dose, and (iii) lack of oxygen inhibition, thereby facilitating the incorporation of cells and biochemical cues [59].

2.3. Hydrogel properties

Hydrogels that exhibit orthogonal control of multiple properties in cellular microenvironment should meet several physical and biological requirements to apply in 3D bioprinting. The main requirement is the biocompatibility of the materials. Biocompatibility refers to the “ability of a material to perform with an appropriate host response in a specific situation" [60]. Also, the hydrogel should be immunocompatible, which does not facilitate significant inflammatory response at *in vivo* microenvironments. Most of the naturally derived polymers including alginate, chitosan, gelatin, hyaluronic acid, and cellulose always show good biocompatibility and few synthetic polymers such as polyethylene glycol (PEG) and its derivatives also demonstrate good biocompatibility in both *in vitro* and *in vivo* conditions. Hydrogels fabricated through the click chemistry, Michael addition reactions, and thiolene reactions using synthetic polymers always generate small molecules such as

unreacted monomers, initiators, and crosslinkers. Therefore, it is essential to remove those byproducts, or it is necessary to select minimal cytotoxic materials in both *in vitro* and *in vivo* microenvironment at the design stage. Apart from biocompatibility, several other factors have to be considered, including mass transport, biodegradability, target microenvironment, mechanical properties, and effect of crosslinking reaction to the cell viability. First considering the mass transport, it is a vital requirement for cell encapsulation, since the continuous exchange of gases (O_2 and CO_2), nutrients, proteins and waste product into, and out of or within the hydrogel is important for viability and proliferation of encapsulated cells. Also, the ability to transfer hydrophobic/hydrophilic molecules is beneficial as some therapeutic techniques requiring controlled drug release (i.e., tumor chemotherapy) [40,58].

Biodegradation is an essential aspect for a biomedical application that requires controlled resorption *in vivo*, and the degradation mainly depends on the bulk dissolution based on several mechanisms such as hydrolysis (ester or enzymatic), photolysis, disentanglement, and combination of these mechanisms [40,58]. The degradation of the material creates more space for cell proliferation, migration, and also for the infiltration of the blood vessels. The development of a spatiotemporal aspect of this type of hydrogel is still a challenge [61,62]. Material-specific degradation will be further discussed in Section 3. However, the ability to mimic the dynamic nature of the ECM is considered as a major challenge in the hydrogel synthesis. The spatiotemporal control of the biological interaction at the material-cell interface including mediate cell proliferation, migration, adhesion, and receptor-ligand binding is challenging due to the complexity of the ECM microenvironment, which includes plethora of structural proteins; such as collagen, laminin, fibronectin, elastin; polysaccharides and various growth factors, enzymes, and inhibitors [58]. This type of biodirectional crosstalk between the microenvironment and the cells is known as “dynamic reciprocity," and multiple tissue engineering approaches have been developed to generate matrices which are capable of this reciprocity [63].

The ability to create a cell-laden hydrogel matrix is greatly dependent on the severity of the crosslinking reaction and the cytotoxicity of the byproducts and unreacted substances. The monomers, initiators, and free radical generated from the reactions can be damaging to the cells, and such effects diminish the efficacy of the 3D microenvironment in both in vitro and *in vivo*. Furthermore, the photoinitiated polymerization reactions which use ultraviolet (UV) radiation or blue light radiation to generate free radicals can be harmful to the encapsulated cells if subjected to the prolonged exposure. Apart from these general properties, viscosity is an essential property for the hydrogels which are subjected to 3D bioprinting or commonly known as the printability of the hydrogel. If viscosity is too high, high pressure should be applied, and the resulting high mechanical forces and shear stresses may damage the cells. In contrast, low viscosity may hamper structural integrity and the resolution of the printed structure [64]. The internal diameter of the nozzle also affects to the post-printing cell viability as a larger diameter nozzle requires low pressure, which subjected to lower shear stress and having good cell viability and *vice versa*.

Another main consideration of developing the hydrogel system is mechanical stability. In some situations, tissue formation can greatly depend on the mechanical properties of the

hydrogels. As an example, the matrices which use in the load-bearing application should withstand until cells have produced their own functional ECM. It is widely known that the mechanical properties of the hydrogel, specifically stiffness, influence the cell adhesion, proliferation, and differentiation. Distcher and coworkers demonstrated that the mesenchymal stem cell differentiates into specific lineages according to the matrix stiffness. Soft matrices that mimic brain meant to be neurogenic, stiffer matrices that mimic muscles became myogenic, and comparatively rigid matrices that mimic collagenous bone prove to be osteogenic [65,66]. However, conventional hydrogels possess low mechanical properties and hence widely used in soft tissue applications. Alternatively, hydrogels, synthesized from hybridization with nanomaterials, by mixing multiple components, or *via* crystallite crosslinking proved to possess good mechanical properties [41]. These techniques will be further discussed in Section 3.

3. Materials for 3D printable hydrogels

3.1. Alginate-based hydrogels

As previously mentioned alginate is a polyanionic, hydrophilic polysaccharide which consists of linear (l-4)-linked β-Dmannuronic acid (M blocks) and its C5-epimer α-L-guluronic acid (G blocks) residues and the G block content varies between 30% and 70% depending on the species and part of the seaweed where alginate is extracted [67]. The M blocks and G blocks are separated by MG regions, and G blocks increase the gel formation while MG and M blocks increase the flexibility of the gel [68]. The presence of divalent cations results in the gelation of the alginate through G blocks because of the affinity for the alkaline earth metals (except Mg^{2+}). The affinity for the cations varies in an increasing manner as $Ca^{2+} < Sr^{2+} < Ba^{2+}$ [69]. Though the gelation process of the alginate in the presence of divalent cations is not fully understood, it is reported that the gelation takes place in an “egg-box" form, where the ions that are locked in between the surrounded pair of helical chains [70]. Pore size, which is in the range of 5 and 200 nm, is an essential parameter related to the cell viability, proliferation, therapeutic drug delivery and it is also crucial for the mass transport such as nutrients, waste products. The largest pore size can be found in the high G block contained alginate. In general, viscosity and elasticity of the gel depending on the concentration of alginate, molecular weight, and the G block content [67,68,71].

Due to the excellent printability and versatility of the material, calcium alginate-based hydrogels are one of the most studied hydrogel systems in the field of 3D bioprinting. Most widely used 3D printing techniques for the alginate-based bioinks are extrusion assisted bioprinting, and the inkjet assisted bioprinting [72]. Natural alginate is a bioinert material with limited degradation [73]. The enzymes that needed to breakdown the alginate polymer chains are not available in mammals and therefore limit the use of alginate for *in vivo* tissue generation [74]. The degradation rate of the alginate was increased in a controllable manner without altering the gelation ability with Ca^{2+} by the Mooney’s group using the oxidation of alginate in the presence of sodium periodate [75]. Ying Mei’s team studied the effect of oxidation percentage of alginate and the viscosity of the solution on human adipose-derived stem cells (hADSCs). According to their findings, 5% oxidation percentage and 10% and

15% (w/v) concentrations of alginate are best for the hADSCs proliferation. The optimal viscosity requirement for the consistent printability of alginate is in the range of 400–3000mm^2 s^{-1} [73]. The increasing viscosity of the alginate adversely affects the cell viability as previously reported in the number of studies [76,77]. Wenmiao Shu's team reported a method to improve the stability of the 3D printed alginate structures by using the three-stage crosslinking method; where partial crosslinking with Ca^{2+} was done to achieve the printability, the second crosslinking with Ca^{2+} was done immediately after the printing for rigidity, and final crosslinking with Ba^{2+} was done for long term stability in the tissue culture media; without significantly altering the cell viability [78].

Making a 3D vascularized structure or organ remains a major challenge in the tissue engineering field. This type of vascularized structure supports cell viability because of enhanced nutrient delivery and oxygen perfusion. A novel coaxial nozzle strategy or core/shell model has been developed in recent years in order to print blood vessel-like microchannels in the cell-laden structures using alginate by Ozbolat's team [79]. The reason for using alginate in this coaxial nozzle strategy was mainly due to their capacity in regulating cell behavior and structural integrity in cell culture. The inner diameter of these nozzles should be carefully selected according to the requirement as the diameter of the microchannels are depending on this factor. In this study, Ozbolat's team selected two coaxial nozzle assemblies: (i) an assembly with 26 gauge (230 μm inner diameter (ID), 457 μm outer diameter (OD)) inner needle and 18 gauge (840 μm ID, 1270 μm OD) outer needle; (ii) an assembly with 23 gauge (330 μm ID, 650 μm OD) inner needle and 18 gauge outer needle in order to understand the effect of wall thickness on cell viability. Later, the same team developed another system to print blood vessel-like channel structure using cartilage progenitor cell encapsulated Ca-alginate gel system [80]. Liang Ma's team developed the same coaxial nozzle method to print microchannels (Fig. 2(a) and (b)) with the addition of external $CaCl_2$ immersion while printing to improve stability. They were able to print different structures (Fig. 2(c)) using perfusable microchannels (Fig. 2(d)) and also they reported the enhanced cell viability in structures with microchannels compared to the structure without microchannels using mouse fibroblast cells [77]. Selvaganapathy's team were able to print hollow channels with a diameter in the range of 500 μm - 2 mm by changing the flow rate or varying the speed of the print heads by using the same method mentioned above [81]. The same coaxial nozzle system was developed to obtain cell-laden core with a mechanically stable shell to create vascular structure known as core-shell model by the Jing Yang's team. This strategy provided several advantages as the cell contained core does not directly expose to the crosslinking agents, and therefore, high cell viability can be obtained. Also, mechanical stability can be achieved by the robust crosslinking of outer shell material [82]. After this method was proposed by the Ozbolat's team, Several studies were done using a different type of hydrogel materials. Those studies will be discussed in the relevant section of hydrogel material.

The incorporation of other natural and synthetic polymers, and inorganic materials into the alginate hydrogels was extensively studied and found enhanced biological and mechanical properties. Nanocellulose was incorporated into calcium alginate hydrogel system deliver the human nasoseptal chondrocytes (hNCs) for cartilage tissue regeneration [83]. Nanocellulose fibers are incorporated to alginate due to their good mechanical properties,

hydrophilicity, and biocompatibility. The compressive stress of the scaffolds was in the range of 25–40 kPa, and the addition of a different amount of nanocellulose did not significantly increase the compressive stress. In another study, Lin Li's team incorporated methylcellulose (MC) into calcium alginate hydrogel system in order to increase the thixotropic property, extrudability, and stackability. The viscosity of the alginate/ MC blend hydrogel system is contributed by the MC, and the viscosity of the hydrogel decreased with increasing shear rate, indicating the shear-thinning behavior. The average compression modulus of the bulk and two-layered alginate/ MC hydrogels were reported as 11.11 and 7.17 kPa respectively. Also, they have used a trisodium citrate treatment to increase the interfacial bonding between printed layers with the presence of mouse fibroblasts, and 95% post printing cell viability was achieved [84]. Gelatin was incorporated into alginate to increase the long term structural integrity with two-step mechanism combining the thermosensitive property of gelatin and chemical crosslinking of calcium alginate. In this study, hydroxyapatite (HA), the main mineral component of the natural bone, was also incorporated into the gel system in addition to the human mesenchymal stem cells (hMSCs, 85% post printing cell viability), where HA favors the use of this hydrogel system for bone tissue engineering. Three different scaffold types - 8% HA, 4% HA, and no HA- were tested for Young's modulus. As expected, Young's modulus of the hydrogel systems increased with the increasing HA content, where 36 ± 3 kPa, 32 ± 2 kPa, and 29 ± 2 kPa of post-printing modulus at day 0 were reported for 8% Ha, 4% HA, and no HA scaffolds respectively. No significant difference was observed at day 3 after swelling, where all the modulus values were around 30–32 kPa range for all three groups [85]. Muller's team reported that bonerelated SaOS-2 cells in the sodium alginate/gelatin hydrogel are in the non-proliferating state. They found out that the addition of an overlay onto bioprinted system consisting of agarose and calcium salt of polyphosphate (Poly.Ca^{2+}) as shown in Fig. 2(e) increases cell proliferation and mineralization of the cell while increasing the Youngs modulus of the scaffold system. Reduced Young's modulus (RedYM) of the alginate system was reported as 2.5 kPa after two day incubation period, and this value further reduced to 0.8 kPa at day 5. The addition of 100 μM of Poly.Ca^{2+} complex increased the RedYM to 22 kPa at 5 day incubation period. However, the presence of SaOS-2 cells in the hydrogel reduced this RedYM value to 3.2 kPa at five-day incubation, indicating the degradation and metabolization of the complex by the cells [86]. In another study, calcium alginate/ polyvinyl alcohol (PVA)/ HA hydrogel system with encapsulation of mouse calvaria 3T3-E1 (MC3T3) cells showed sufficient integrity and mechanical properties over 14 days incubation period without diminishing the cell viability [87].

Kim's team reported the alternative printing layers of poly (ε caprolactone) (PCL) and MC3T3 cell encapsulated calcium alginate hydrogel system showed significantly improved mechanical properties and 84% of cell viability after 25 days of cell culture. Two different scaffold orientations were made as one alginate strut between PCL struts, and two alginate struts between PCL struts. Tensile modulus values were completely dependent on the PCL strut volume fraction, where 15.4 MPa and 8.3 MPa tensile modulus values were reported for high PCL struct volume scaffold and lower PCL struct volume fraction scaffolds respectively [88]. Calcium alginate containing transforming factor-β (TGF-β) and chondrocytes were printed using a layer by layer technique with the combination of PCL by

Cho's group, where enhanced cartilage tissue and type II collagen formation was observed in both *in vitro* and *in vivo* experiments. Mechanical stability of the scaffold was achieved through the PCL, and alginate acted as a cell carrier [89]. Bone morphogenic protein-2 (BMP-2) loaded gelatin microparticles incorporated calcium alginate scaffolds showed enhanced osteogenic differentiation and the controlled release of BMP-2 in the goat multipotent stromal cell (gMSCs) encapsulated system. Gelatin microparticles (MPs) are suitable for BMP-2 delivery, where 30% of the BMP-2 shows burst release at the beginning and the remaining amount released in a controlling manner due to the enzymatic degradation of the gelatin. The presence of BMP-2 in gelatin MPs led to osteogenic differentiation *in vitro* and *in vivo*, and higher release of BMP-2 was observed *in vivo* conditions due to the higher enzymatic activity. However, after 4 weeks of subcutaneous implantation of the scaffolds in mice, BMP-2 was still available in the implanted scaffolds [90]. Ouyang's team developed alginate/HA scaffolds having an anti-inflammatory function via the addition of atsttrin; a progranulin derived engineered protein, to reduce the effect of proinflammatory tumor necrosis factor- α (TNF-α). High expression of TNF-α adversely affects to the BMP-2 induced osteoblastic differentiation, and atsttrin exerts an antagonistic effect on TNF-α function [91].

3.2. Collagen-based hydrogels

Collagen is one of the major components in all the connective tissues, making one of the most studied biomolecules of the ECM, with a triple helix structure. Collagen represents approximately 25% of the total dry weight of mammals [12,92]. Even though collagen can be extracted from almost every living animal, the source for tissue engineering applications include porcine skin, bovine skin and tendons, and rat tail among others. Collagen types I, II, III, V, and XI are only known for making collagen fibers out of 29 distinct collagen types up to date. Apart from all the collagen types, type I collagen (Col-I) is the mostly (only) studied collagen type in 3D bioprinting due to its ability to undergo self-assembly to form fibrous hydrogels [93]. Type I collagen stays in liquid form at low temperatures while increasing temperature (37ºC) or remaining at neutral pH forms fibrous hydrogels. However, Col-I has an intrinsic limitation due to the slow gelation, whereas it takes half an hour to form gel at 37 °C. Because of this slow gelation, the required structural stability cannot be achieved after bioprinting. Also, the slow gelation reduces homogeneity of the cells in the hydrogel, since the cells move downwards and stabilize in the bottom due to the gravity. So, collagen cannot be used alone without a support material due to its weaker mechanical properties and slow gelation rates. Several studies were reported the successful incorporation of collagen into a different type of natural and synthetic hydrogel systems.

Cho's team developed a 3D structure which mimics the osteochondral tissue by incorporating human chondrocytes, derived from human septal cartilage, and osteoblasts (MG63 cells), derived from human osteosarcoma. They studied the overall behaviors of chondrocytes and osteoblasts on Col-I and alginate-based hyaluronic acid (HLA) gel system. Both chondrocytes and osteoblasts were better in their native ECMs, HLA, and ColI respectively. HLA, mixed with alginate and then crosslinked with $CaCl_2$, has shown Young's modulus of 21.4 ± 5.7 kPa. Col-I, crosslinked by increasing temperature, has shown Young's modulus of 4.3 ± 1.4 kPa. Chondrocytes encapsulated collagen hydrogel system, and

osteoblasts encapsulated HLA/ alginate hydrogel system had shown 90% of cell viability and growth up to 14 days *in vitro* for osteochondral tissue generation. [94].Hyung Kim's team investigated the previously mentioned core/shell model to encapsulate hADSCs in the core with collagen hydrogel, and the shell of calcium alginate without cells using a coaxial nozzle system. Collagen is a good cell carrier because of its role as a natural ECM material, but due to its weak stability and prolonged crosslinking time diminish the ability to use Col-I as a 3D printable hydrogel. In this study, Col-I was covered with a calcium alginate shell, which gives mechanical support during the printing process [95]. High-density collagen hydrogel was used to overcome the low mechanical stability of the construct by Bonassar's team. The equilibrium compression modulus of the printed tissue constructs increased linearly with increasing collagen concentration and 2 fold increase of modulus was observed from 10 mg/ml to 20 mg/ml collagen concentration. Modulus of 30kPa was obtained at the highest printable collagen concentration of 17.5 mg/ml, where 20 mg/ml concentration was not suitable due to the clogging and precross-linked of the collagen inside the tip. They have reported good cell viability and maintained cell growth of primary meniscal fibrochondrocytes for cartilage repair. Cell viability of the printed construct did not significantly vary with the density of the collagen (from 12.5 mg/ml to 17.5 mg/ml), and no reduction in the cell viability was observed over 10 days in culture [96]. The same team studied the effect of riboflavin photocrosslinking through blue light, and the effect of pH on the primary articular chondrocytes encapsulated Col-I-based hydrogel system. However, the cell viability approximately decreased from 95% to 75% due to the addition of blue light-activated riboflavin crosslinking [97]. The reduction of cell viability was due to the addition of higher concentration of riboflavin (0.5 mM) and as previously reported, 0.25 mM of riboflavin was the optimum concentration to prevent the reduction of cell viability. In contrast, low concentration reduces the mechanical stability of the hydrogel while blue light-activated crosslinking also reduces the cell viability [98]. Soker's team developed an *in situ* 3D bioprinting technology to treat a full-thickness skin wound in nu/nu mice using fibrin-collagen gel system. They reported that the amniotic fluid-derived stem cells (AFSCs) treated wounds have shown enhanced microvessel density and capillary diameter compared to the bone marrow-derived stem cells treated wounds [99]. Boland's team developed a 3D printed fibrin-collagen I based dermo-epidermal graft for skin wound using the ink-jet printer. Three types of cells, namely neonatal human dermal fibroblasts, human dermal microvascular endothelial cells, and neonatal human epidermal keratinocytes were encapsulated into the hydrogel system and near identical to natural skin of athymic nude mice with microvessels was obtained [100]. Similarly, Reimers's team developed laser-assisted bioprinting (LaBP) to coat a thin layer of fibroblasts and keratinocytes encapsulated collagen hydrogel system on top of the stabilizing matrix (Matriderm®) for full-size skin wound in nude mice [101]. Recently, collagen was incorporated into sodium alginate gel system to deliver the chondrocytes without altering the gelling mechanism of sodium alginate. They have made porous scaffolds; which are having good post printing resolution; with sodium alginate, sodium alginate with agarose, and sodium alginate with collagen type I as shown in Fig. 2(f)[102]. Collagen type I and macromolecule-based polyvinylpyrrolidone (PVP) bioink was developed to deliver fibroblasts using a novel single step drop on demand (DOD) bioprinting strategy [103].

3.3. Chitosan-based hydrogels

Chitosan, a natural cationic copolymer of β-(l-4) linked 2-acetamino-2-deoxy-D-glucopyranose and 2-amino-2deoxy-Dglucopyranose, is a deacetylated form of chitin derived from shells of crustaceans [104,105]. Cell-laden 3D printed structure using chitosan-based hydrogels are not extensively studied due to the acidity of the gel. Chitosan dissolved only in the weak acids such as acetic acid, and the pH (around 4.0) of the solution is not favorable for living cells. Several studied were performed to encapsulate cells in the chitosan-based scaffolds using different techniques such as mixing with other natural and synthetic hydrogel systems and neutralizing the pH. Recently, one research group was able to print cell-laden chitosan-based scaffolds using a glycerol phosphate disodium salt as an ionic crosslinker while adding NaOH to increase the pH up to 7.0 after dissolving the chitosan in acetic acid. They incorporated HA and MC3T3-E1 cells with the chitosan gel and compared to the cell viability and differentiation of alginate/HA scaffolds. Enhanced cell functions were reported in the chitosan/ HA hydrogel compared to the alginate/ HA gel system [106]. Jia-Kuo Yu's group developed a thermoresponsive chitosan gel system by mixing the chitosan which dissolved in 0.1 M acetic acid with a βglycerolphosphate solution. This system remains in the liquid form at 4ºC starts sol-gel transition at 37 °C. This team developed a hybrid scaffold with PCL to deliver BMP-2 and the rabbit bone marrow derived MSCs in to a mice cranial defect. The compressive strength of the chitosan thermoresponsive gel, and PCL incorporated hybrid system was reported as 200 kPa, and 6.7 MPa (similar to human cancellous bone) respectively [107]. It was reported that the pore size greater than 300 μm are beneficial for enhanced angiogenesis and osteogenesis, while small pores favored hypoxic conditions and would induce chondrogenesis [107,108]. Several authors have reported the use of carboxymethyl chitosan, water soluble chitosan derivative, as a successful candidate to make cell-laden 3D printed scaffolds with the combination of other natural or synthetic polymers [109].

3.4. Hyaluronic acid-based hydrogels

Hyaluronic acid (HLA), a linear non-sulfated glycosaminoglycan (GAG), is a polysaccharide with the repeating disaccharide, β-1,4D-glucuronicacid, β-1,3-*N*-acetyl-D-glucosamine [21,110]. HLA is a major ECM component of cartilage and ubiquitously find in almost all connective tissues. To use HLA as a 3D printable bioink, chemical modifications and mixing with other polymers are often carried out to enhance the rheological and mechanical properties. HLA and gelatin-based gel system with human cardiac-derived progenitor cells (hCMPCs) were used to print a cardiac patch, which has shown enhanced cardiac and vascular differentiation in a mouse model. As shown in Fig. 2(g), very high post-printing cell viability, and homogeneous distribution of the hCMPCs were obtained. [111]. Doyle's team developed a thermoresponsive HLA and MC blend to deliver sheep adipose-derived mesenchymal stem cells [112]. Rajaram's team investigated the addition of polyethyleneimine (PEI), a polycation which stabilizes the alginate molecular structure through the formation of polyelectrolyte, into the HLA/alginate hydrogel with ATDC-5 chondrogenic cells. They have found reduced cell viability with increasing PEI concentrations, and Young's modulus of the 0.1% PEI and 0.5% PEI scaffolds were reported as 1.4kPa and 1.6kPa respectively [113]. Burdick's team developed a methacrylated HLA (MeHA), which facilitates the UV photocuring through the addition of 4-(2-

hydroxyethoxy)phenyl(2-propyl)ketone (Irgacure 2959) photoinitiator. The stability of the hydrogel system further enhanced through the guest-host mixture, where adamantine act as a guest and β-cyclodextrin as a host, separately coupled to the MeHA mixture [114]. The use of HLA in the other polymer based hydrogel systems will be discussed in the appropriate sections.

3.5. Gelatin and methacrylated gelatin-based hydrogels

Gelatin, a partially hydrolyzed form of collagen, is a water soluble and biodegradable polypeptide. The gelling properties of the gelatin depend on the origin of the source, such as mammalian derived gelatin, fish-derived gelatin. The use of gelatin in tissue engineering applications is limited due to its higher enzymatic degradation rates and poor mechanical stability because of the high solubility in the physiological environment [115]. Several studies were done on gelatin only scaffolds, but the prolonged crosslinking period at extreme conditions have restricted the use of cells [116,117]. However, gelatin-based hydrogels have been extensively studied in the field of tissue engineering by incorporating natural and synthetic polymers, and inorganic materials to increase the stability of the system. Butcher's group developed calcium alginate and gelatin-based hydrogel system to develop valve conduits, which can deliver dual cell types in a region-specific manner, with anatomical architecture. They incorporated aortic root sinus smooth muscle cells (SMCs) and aortic valve leaflet interstitial cells (VICs) in the alginate/gelatin gell system. The mechanical stability of the gel system reduced over time in the cell culture media, where ultimate tensile strength of cell-free hydrogel reduced from 0.84 ± 0.07 MPa to 0.40 ± 0.04 MPa after 7 day immersion, and elastic modulus decreased from 1.44 ±0.3 MPa to 0.96 ±0.08 MPa at 7 day immersion [118]. In another study, compressive modulus of the alginate/gelatin hydrogel was reported. The increasing concentrations of alginate and gelatin increased the compressive modulus while reducing the cell viability due to the higher pressure and shear stress subjected to the cells during extrusion-based bioprinting. The compression modulus of the 5% (w/v) alginate/6% (w/v) gelatin and 7% alginate/ 8% gelatin were reported as 29.8 ± 2.49 kPa, and 48.0 ± 5.74 kPa respectively [119]. Shah's team investigated a multi-polymer hydrogel system based on gelatin. They have developed 35 formulations of extrudable bioink systems with multi crosslinking, consist of gelatin type A, gelatin methacrylate, fibrinogen, and modified PEG (amine-carboxylic coupling; PEGX, X = sucinimidyl valerate) by changing the composition of each material and varying the crosslinking degree. They have incorporated hMSCs, human dermal fibroblasts (hDFs) and TGFβ into the gel, and 2-hydroxy-4-(2-hydroxyethoxy)-2-methylpropiophenone was used as the photoinitiator for gelatin methacrylate [120]. The teams lead by the Atala have developed several hydrogel systems based on gelatin and various synthetic and natural polymers. A hydrogel consists of glycerol, fibrinogen, gelatin, and HLA with the addition of Pluronic F-127 as a sacrificial material, and PCL as a supporting material was used to bioprint various vascularized tissue construct with various cell types. C2C12 myoblasts encapsulated skeletal muscle construct, hAFSCs encapsulated human mandible bone structure, and rabbit primary auricular chondrocytes laded human ear structure were successfully fabricated using the extrusion-based integrated tissue-organ printer (ITOP) [121]. Similarly, HLA and gelatin-based hydrogel system were developed with two crosslinkers and 2 stage polymerization [122]. They have developed various bioink formulation systems consist of thiol-modified gelatin

(Gelin-S), thiol-modified HLA (Heprasil), PEG diacrylate (PEGDA), 4-Arm PEG acrylate, 8-Arm PEG alkyne, 4-Arm PEG alkyne, Irgacure 2959 as a photoinitiator, and unmodified gelatin and HLA was added to improve the shear thinning and extrusion properties (Fig. 3 (a)). This bioink system was used to incorporate primary human liver hepatocytes (as liver spheroids) (Fig. 3(b)), a well known cell type for its difficulty to maintain *in vitro*.

Methacrylated gelatin was first introduced in early 2000 by Etienne H. Schacht and coworkers and known as gelatin methacrylamide [123]. The addition of functional groups to the gelatin backbone increases the degree of control of hydrogel design and properties through a crosslinking process, which either uses photoradical initiation or enzymatic crosslinking. Most of the reported literature used photo-initiated radical formation as it provides more temporal and spatial control over the enzymatic crosslinking process [124,125]. Substitution of the amine groups in gelatin can be done by using several chemicals, such as methacrylol chloride, glycidyl methacrylate, methacrylic anhydride, but the use of methacrylic anhydride is the most efficient process and resulting in a more stable product [126]. Therefore, the most widely used method for synthesizing methacrylated gelatin is the mixing gelatin with the methacrylic anhydride, but the final product is being called by three different names, gelatin methacrylate, gelatin methacrylol, and gelatin methacrylamide, and used same acronym GelMA.

After 2010, GelMA is extensively using as a 3D printable bioink for different tissue engineering applications with the incorporation of different cell types. It is reported that 5–15% (w/v) concentration of GelMA hydrogel can support the cell spreading and 7–15% (w/v) of GelMA is required to achieve successful bioprintability with hepatocarcinoma (HepG2) cells and NIH 3T3 Cells by using extrusion-based printing [127]. Khademhosseni's group extensively studied the use of GelMA in tissue engineering applications using Irgacure 2959 as a photoinitiator. The compressive modulus of the GelMA depends on the methacrylation degree and the concentration of the GelMA, where the compressive modulus of GelMA with higher methacrylation degree was reported in the range of 5–30 kPa from lower concentration to higher concentration respectively [128]. In another study, they have reported that the degree of methacrylation of GelMA can be used to modulate the cellular behavior and the extent of vascular network formation both *in vitro* and *in vivo*. Also, the cell spreading, organization, and proliferation depend on the methacrylation degree, where softer hydrogels, with lower methacrylation degree, are more lenient than the stiffer hydrogels, with higher methacrylation degree. 1 M GelMA showed superior vascularization than 10 M GelMA when encapsulated with human blood-derived endothelial colony-forming cells (ECFCs). Monoculture of ECFCs was not able to proliferate or spread in GelMA while coculture with hMSCs showed spreading of ECFCs [129]. In a recent study, a novel strategy to bioprint cell-laden GelMA in lower concentration (3%) was proposed using GelMA physical gels (GPGs), where the GelMA was subjected to the cooling process (4° C) before printing [130]. As expected, the viability of the human umbilical vein endothelial cells (hUVECs) was reduced with increasing GelMA concentrations. In another study, a novel hybrid strategy to fabricate endothelialized myocardium on-a-chip platform was investigated using a mixture of GelMa and sodium alginate with hUVECs. Previously described coaxial nozzle method was used to print hollow tubular structure with the incorporation of the two steps crosslinking as shown in Fig. 3(c),

where $CaCl_2$ was delivered through the core of the nozzle to crosslink the alginate component of the gel mixture ionically. After printing, post-crosslinking was done using UV light for the 30 s, and human-induced pluripotent stem cells (hiPSCs)-cardiomyocytes were seeded to the scaffold. The scaffolds with different aspect ratios were printed, as shown in Fig. 3(d), and fluorescent microbeads were added to the bioink to distinguished the distance between microfibers. The system was kept in the microfluidic perfusion bioreactor and proposed to use as a platform for cardiovascular drug screening. The perfusion greatly affects the viability of both hUVECs and hiPSCs-cardiomyocytes, as shown in Fig. 4(a)–(d) [131].

Dubruel's team investigated the use of photoinitiator, 2–2'azobis[2-methyl-*N*-(2-hydroxyethyl)propionamide] (VA-086) as a substitution for conventional Irgacure 2959 photoinitiator. The porous scaffold structure was bioprinted with HepG2 cells using 10% (w/v) GelMA without adding viscosity-enhancing additives. More than 97% of cell viability was obtained with VA086 photoinitiator (Fig. 4(e) and (f)), and the maintained expression of liver-specific functions was observed [132]. Instead of 365 nm UV irradiation, Kim's team proposed quick blue light laser photocuring at 405 nm wavelength using VA-086 due to the high cell viability after crosslinking compared to the Irgacure 2959, which can not be activated at wavelengths above 370 nm. The optimum cell viability was achieved through 250 mW laser power and 10 s crosslinking time using 10% GelMA. Over 90% cell viability of NIH 3T3 cells was reported at day 0 post-printing, and cells elongated inside the microenvironment of gel at 2 days of culture [133]. Chen and the coworkers developed a patient-specific hepatic model to personalized *in vitro* drug screening, and disease study with the incorporation of hiPSC derived hepatic progenitor cells (hiPSC-HPCs) using a stereolithography technique based on a custom-built digital micromirror device (DMD). Methacrylated HLA (GMHA), a product synthesize through the reaction of HLA with glycidyl methacrylate, and GelMA were used as bioinks with a photoinitiator, lithium phenyl-2,4,6-trimethyl benzoyl phosphinate (LAP) [134]. In a recent study; two steps crosslinking strategy, rapid reversible crosslinking of gelatin, and irreversible photocrosslinking of GelMA; was used to achieve the printability through the reduction of GelMA concentration, which adversely affects to the cell viability and spreading of cells. In this method, they were able to print viscosity similar to 30% (w/v) GelMA, using 5% GelMA and 8% gelatin, without affecting to the cell viability and mechanical stability [135].

The main concern related to the GelMA hydrogel is the poor mechanical strength, which adversely affects the load-bearing applications such as bone and cartilage repair. To address this problem, several methods have been used, including alternated printing with PCL and making a support structure using thermoplastic materials. In one study, reinforced cell encapsulated GelMA soft hydrogel with organized high porosity microfiber network of PCL was investigated. The hydrogel was later printed to the etched PCL fiber network, where etching with NaOH increases the stiffness of the composite and more responsive to the mechanical loading. Instead of photocrosslinking, a combination of two chemical crosslinkers ammonium persulfate/tetramethylenediamide (APS/TEMED) was used to stabilize the gel. The stiffness of the GelMa crosslinked with 12.5 mM, and 25 mM APS/TEMED was reported as 7.1 ± 0.5 kPa and 7.5 ± 1.0 kPa respectively. The stiffness of the porous PCL hydrogel composite scaffolds was significantly increased to 214 ± 24 kPa and

405 ± 68 kPa in 12.5 mM and 25 mM APS/TEMED crosslinked sample respectively. Human chondrocytes were incorporated to the GelMA/APS mixture before crosslinking, where over 80% of cell viability was achieved at day 1, and cell viability closer to the 80% also maintained up to 7 days of culture [136]. Malda's team also investigated the alternating printing of PCL, as a supporting material, and a mixture of GelMA and HLA hydrogel, where HLA acts as a viscosity enhancer, encapsulated with chondrocytes. They have reported cartilaginous matrix formation at 4 weeks and improved mechanical moduli (5–180 kPa) [137].

3.6. Poly(ethylene glycol) (PEG) based hydrogels

PEG is one of the most widely studied hydrogels in tissue-engineered scaffolds for cell studies and drug delivery [138]. PEG is a hydrophilic, biocompatible, and nonimmunogenic polymer due to its intrinsic molecular structure, where PEG diol surround with two hydroxyl end groups, which can be converted into other functional groups such as carboxyl, methoxyl, thiol, amine, vinyl sulfane, azide, acetylene, and acrylate [139,140]. Photopolymerization is the most common strategy to make PEG hydrogel, which allows more spatial and temporal control for the fabrication of scaffolds *in situ*. PEG diacrylate (PEGDMA), PEG dimethacrylate (PEGDMA). and multiarm PEG acrylates (n-PEG-Acr) are the major type of PEG macromers used in photopolymerization to PEG hydrogels, which are not naturally biodegradable. The addition of degradable segments, including poly (propylene fumarate) (PPF), polyester, acetal, and disulfide enhances the degradation rate of PEG-based hydrogels.

Prestwich and the co workers investigated the use of tetrahedral PEG tetracrylates (TertraPACs) in cell encapsulation. They were able to bioprint a vessel like constructs using thiolated HLA crosslinked with TetraPACs, where NIH 3T3 cells were encapsulated, by adding the agarose microfilaments, as shown in Fig. 5(a) and (b). Two 4-arm PEG derivatives with different PEG chain lengths (TetraPEG8 and TetraPEG13) were synthesized from tetrahedral pentaerythritol derivatives.This PEG hydrogel has shown significantly high shear modulus compared to the PEGDA hydrogel and good cell viability up to 4 weeks [141]. In another study, a perfusable construct with a hollow interior vessel-like structure was developed using a multilayered coaxial extrusion system. The hydrogel system consists of GelMA, sodium alginate, and 4-arm PEG-tetra acrylate (PEGTA) with the addition of hUVECs and hMSCs. The hollow structure was achieved through the initial ionic crosslinking with the Ca^{2+} (flows through core nozzle) during the printing, and the final covalent photocrosslinking of GelMA and PEGTA was done after printing (Fig. 5(c)). The varying diameter of hollow tubes were printed by changing the diameter of nozzles, as shown in Fig. 5(d). Significantly higher compressive modulus was observed with compared to that of GelMA only scaffolds as increasing PEGTA concentration increased the modulus, where 50.7 ± 3.0 kPa compressive modulus was observed in 3% (w/v) PEGTA scaffolds. Fig. 5(e) shows a printed structure before and after perfusion, and this technique can be used to print continuous hollow tubes with complex shapes (Fig. 5(f)) and also hollow tubes with varying diameters (Fig. 5(g)) [142]. Bertassoni's group developed a perfusable microchannel system in different PEG derivatives using agarose as a removable material to create microchannels. These microchannels were successfully embedded in to GelMA, star PEG-

co-lactide acrylate (SPELA), PEGDMA, and PEGDA based hydrogel systems, but the cell encapsulation was only done in GelMA system, where MC3T3 cells were mixed with GelMA and hUVECs were injected to the created microchannels, and successful completion of endothelial monolayer was observed [143].

A eosin Y based photoinitiator, 2',4',5',7'-tetrabromflurescein disodium salt, was used to make covalent bonds in a hydrogel mixture of GelMA and PEGDA through a visible light (514 nm) radiation, where 85% of NIH 3T3 cell viability was observed up to 5 days [144]. Xiaofeng Cui's team developed a number of 3D printed (inkjet-based) PEG-based hydrogel systems to be used in bone and cartilage tissue engineering. In one study, nanoparticles of bioactive glass (BG) and HA were separately incorporated into the PEGDMA hydrogel to investigate the effect of BG and HA on cell viability and mechanical strength. Highest cell viability (86.62 ± 6.02%) of hMSCs was observed in HA incorporated PEGDMA hydrogel, and alkaline phosphatase activity (ALP) and gene expression by quantitative PCR was shown that PEGDMA-HA was better compared to the PEGDMA-BG group [145]. Also, in another study, acrylated arginylglycyl-aspartic acid (RGD), and acrylated matrix metalloproteinase (MMP) sensitive peptide were synthesized and incorporated into the PEGDMA hydrogel system with hMSCs. Hydrogel with PEG peptides showed high expression of collagen type X and MMP13, and the system strongly stimulated the endochondral bone formation [146]. A mixture of PEGDMA and GelMA showed 80% cell viability of encapsulated hMSCs and enhanced osteogenic and chondrogenic expression were shown in PEGDMA/GelMA system compared to PEGDMA alone system [147]. Kaplan's team studied the incorporation of the physical gelation of silk fibroin protein at 37°C to 3D bioprinting with PEG. They have found that the system was compatible with the hMSCs and surprisingly, higher silk concentration gels (10%) supported the better cell growth than lower concentration gels. Mouse fibroblasts encapsulated scaffolds were subcutaneously implanted in the mice, and the scaffolds maintained the shape and structure after 6 weeks while maintaining the viability of a significantly higher number of cells [148]. In a recent study, PEG microgels were prepared via off-stoichiometry thiol-ene click chemistry using 4-arm PEG-norbornene (PEG-Nb) and PEG-dithiol (PEG-DT). The microgels were prepared using electrospraying technique, and the PEG-Nb encapsulated with hMSCs were printed using an extrusion-based printer, where LAP and PEGDT were added to the printed structure to photocrosslinking [149]. Ligler's team developed a bio/synthetic interpenetrating network ($BioSIN_x$) containing GelMA and PEG, where GelMA polymerized within a PEG framework. The PEG network was formed by thiolyne coupling, and GelMA was integrated using a thiol-ene coupling reaction. The schematic representation of the reactions is shown in Fig. 6. They successfully made microfilament encapsulated with endothelial cells by using the hydrodynamic method. This hydrogel system can be successfully developed into a 3D bioprintable bioink [150]. The summary of advantages and disadvantages of each hydrogel type we have discussed in this section is shown in Table 2.

4. Recent trends in bioprinting technology

4.1. Scaffold-free bioprinting

The scaffold-based bioprinting has been explored widely in the past decade, where scaffold-based tissue construct provide mechanical and molecular cues to promote cell adhesion, cell proliferation, and promote ECM production [151]. However, there are several adverse effects created by the polymers and exogenous matrix-based tissues, such as necrosis at the tissue core due to the poor nutrient diffusion *in vivo*, interfere with direct cell-cell interaction, and toxic degradation products [23,151,152]. Because of the reasons mentioned above, as an alternative, 3D printing based scaffold-free tissue engineered construct have been explored. To eliminate the creation of 2D monolayer and cell-substrate interference, low (or none) adherence substrate or plates or hanging droplets can be utilized [72]. The cardiac patch was created using cardiomyocytes, endothelial cells (both human umbilical vein and embryonic stem cell-derived endothelial cells), and fibroblast to avoid core necrosis *in vivo*, where low attachment plates were used *in vitro*. The patches survived in implantation *in vivo*, and the performed human microvessels anastomosed with the rat host coronary circulation [152]. In another study, the non-adherent substrate was used to create vascularized human liver-like tissue structure with human induced pluripotent stem cells (hiPSCs) [153]. The liver buds created *in vitro* were transplanted into the mice became functional within 48 h by connecting to the host vessels.

Scaffold-free bioprinting is explored to synthesized hollow tube structures where vascularization is required. Scaffold-free vascular construction was printed layer by layer with agarose rods, used as a non-adhering molding template (Fig. 7(a)). Human skin fibroblasts (HSF) and human umbilical vein smooth muscle cells (hUVSMCs) aggregated into discreet units either as multicellular spheroids or as cylinders of controlled diameter (Fig. 7(b)). Also, multicellular cylinders composed of hUVSMCs and HSF were made, as shown in Fig. 7(c) [23]. In another study, low adherent agarose mold was used to print tissue spheroids, make from alginate-based microdroplets, containing endothelial cells and smooth muscle cells. It is reported that the cell-secreted collagen type I plays a critical role in promoting cell-cell adhesion, tissue formation, and maturation [151]. Overhang structure of sodium alginate hydrogel was successfully fabricated using inkjet printing with fibroblasts (3T3 cells), where this method can be applied to make blood vessels [154]. The conventional coaxial nozzle system also can be used to make scaffold-free bioprinted structures. Articular cartilage tissue strands were made using alginate-based hydrogel system with the ability to assemble into different shapes [155]. Apart from vessel-like structures, laser-assisted tissue graft was printed using alginate and ethylenediaminetetraacetic acid (EDTA) with porcine-derived MSCs, where good osteogenic and chondrogenic differentiation was observed after culturing *in vitro* [156].

4.2. Four-dimensional (4D) bioprinting

4D printing inspired by the natural shape morphing systems, such as nastic plant motions; where external environmental stimuli, including humidity, light or touch causes a shape change in leaves, flowers, bracts and tendrils [157]. Simply, a fourth dimension, time is introduced to the 3D printed structure; where their shape and or function can change over

time due to an applied external stimuli, such as moisture [157], light [158], temperature [159], pH [160], magnetic field [161], or electric impulse [162], 4D printing is considered as printing of stimuli-responsive material, known as a smart material, that can be physically or chemically changed in response to external stimuli [72]. In addition to the above definition, the 4D bioprinting is considered as the printing of microengineered tissue construct with the cells, where the time dimension that is related to maturation of tissue construct through self-organization of the cellular process such as cell communication and cell interaction, plays a significant role [163]. Shape memory polymers and the hydrogels are the best candidates used in 4D bioprinting [72,163]. Up to date, cell encapsulated 4D bioprinting is not widely studied, and, therefore, here we will discuss some of the new natural and synthetic hydrogel system used in 4D printing in recent years with the addition of cell encapsulated 4D bioprinting. This stimuli-responsive shape morphing of the hydrogels categorized into different sections based on stimuli such as temperature-responsive shape morphing, moisture responsive shape morphing, magnetic field-responsive shape morphing, and light-responsive shape morphing.

Several researchers have investigated temperature-responsive shape morphing hydrogel systems in recent years. A nanocomposite hydrogel consists of poly (*N*-isopropylacrylamide) (PNIPAM), and synthetic hectorite clay undergoes a fluid-gel transition in response to the temperature increment up to 80ºC due to the phase transition [159]. PNIPAM is widely used in thermo-responsive shape morphing systems. Alginate and PNIPAM based hydrogel system were used to make a hydrogel that exhibits a large reversible volume transition at the critical temperature, T_c (=32 to 35 ºC) [164]. In a recent study, Laponite, a synthetic clay, was used to synthesize thermo-responsive hydrogel through mixing that with agarose and acrylamide, where physical crosslinking of agarose and photocrosslinking of acrylamide give the stability to the hydrogel (Fig. 8(c)). Laponite increases the shear-thinning properties and stability of the post-printing structure and also showed higher mechanical properties compared to agarose only and acrylamide only gels [165].

Moisture-responsive shape morphing in 4D bioprinting was first investigated by the Galdman's team. They have found that the orientation of the printed layers affected the self-folding direction after subjected to swelling, as shown in Fig. 8(a) and (b)[157]. Because of the physiologically appealing conditions in moisture-responsive shape morphing, most of the cell-laden scaffolds response to moisture or swelling. The swelling dependent shape-morphing hydrogel was developed using the PEG bilayer, where PEG with two different molecular weights was printed in bilayer form. Swelling of the two PEG sections was different, and the shape change was occurred due to the different swelling ratios of the PEG bilayers (Fig. 8(d)). Cylindrical hydrogel structures of different radii were prepared with encapsulation of insulin-secreting β-TC-6 cells using this method [166]. Selffolding hydrogel-based tubes were developed using methacrylated alginate and methacrylated HLA with mouse bone marrow stromal cells, where cell survival up to 7 days was observed [167]. This type of self-folding hydrogels can be used to make cell-laden vascular structures. Recently, one research team developed bioinspired robots, where self-actuating cardiac muscles integrated on a hierarchically structured scaffold with flexible gold (Au) microelectrodes. This microinspired soft robot consists of four layers; (i) PEG hydrogel

layer gives mechanical stability while facilitating easy deformation under cell contraction and relaxation, (ii) flexible Au electrodes facilitate precise control and efficient electrical signal propagation, (iii) carbon nanotube - GelMA hydrogel gives the suitable microenvironment for cardiomyocyte culture and alignment, (iv) seeded neonatal rat cardiomyocytes layer. After maturation, the cardiomyofiber organization was observed leading to the self-actuating movement [168].

However, there are still some challenges associated with 4D bioprinting techniques. Cells can affect the responsiveness of stimuli-responsive materials, and also, cell viability can be reduced due to the material dynamics [169]. Furthermore, the interaction of the 4D bioprinted structures with native microenvironment (or *in vivo*) should be further studied. Most of the current stimuli-responsive materials respond only to one type of stimulus, but cellular activities in the body are complicated and controlled by multiple stimuli, such as humoral regulation, self-regulation, neuro-regulation [170]. Therefore, 4D bioprinted constructs that can respond to the multiple physiological cues are advisable for use in tissue engineering applications. The expansion and advancement in the nanobiomaterials and nanotechnology research area would inbreed the smart materials that are capable of interacting with the cells and tissues in the cellular and molecular level and further, facilitate the development of 4D bioprinting.

4.3. 3D bioprinting of organ-on-chip systems

Organ-on-chip systems are emerging as a versatile tool in biomedical applications that can be used to reproduce the complex tissue microenvironment by introducing cells into a microfluidic device, which reproduce organ-level functions [171–173]. This microfluidic device acts as a bioreactor, where cells can be engineered by reproducing the biomimetic stimuli such as chemical cues and dynamic mechanical cues to the micro-engineered tissue construct [173]. The development of a complex 3D micro-organ system using conventional fabrication techniques such as lithography and gel confinement has a limited capability. However, the development of 3D bioprinting techniques makes a path for the rapid development of lab-on-chip systems due to its ability to construct complex shapes using layer-by-layer with a high precision cell deposition. After the emergence of 3D bioprinting technology, a board variety of tissue models were studied *in vitro*, such as lung, heart, liver, kidney, skin, and muscle [174]. In this paper, we will discuss recent researches related to bioprinting of organ-on-chip systems.

Fischer’s team developed a perfusable blood vessel model using the drop-on-demand bioprinting technique. Three types of cells were incorporated into the hydrogel materials, where gelatin with hUVECs, and human dermal fibroblasts (hDF) in the core, fibrinogen, and collagen mixed with human umbilical artery smooth muscle cells with hDF in the middle, and collagen and thrombin as a crosslinker with hDF in the outer layer. This group utilized a custom build three printheads for bioprinting, and gelatin was selected as a sacrificial material to make hollow vessel structure. Furthermore, 83% of smooth muscle cell viability was observed, and the expression of cadherin, smooth muscle actin, and collagen IV were observed throughout the culture period [174]. We introduced another two vascularization methods in the previous sections. In one method, the coaxial (core/shell)

method was used to make a vasculature structure using GelMA and alginate hydrogel mixture, where $CaCl_2$ core made the hollow structure [131]. Also, Bertassoni's group studied the PEG-based derivatives and GelMA to make perfusable microchannels by incorporating agarose [143]. However, all the above-mentioned systems have thin vascularized tissues and limited culture times. The typical vascularized structure should have bulk transfer of fluid throughout the organ-on-chip, and therefore dense vascularized system is required to endure thick organ-on-chip system for a more extended time [175]. Lewis's team developed a thick vascularized tissue (1 cm), which can be actively perfused with growth factor for long duration (>6 weeks). In this method; multiple cell-laden, fugitive, and ECM inks were coprinted within 3D perfusion chips under ambient conditions. The customized perfusion chips were created on glass substrate using silicone ink. Then; fugitive ink, Pluronic-127 sacrificial material was printed in crosshatched pattern, and later, cell-laden bioinks, which contain gelatin and fibrinogen with hUVESs, hDFs, and hMSCs were 3D bioprinted around the crosshatched pattern. The crosslinkers of the fibrinogen; thrombin and transglutaminase, which cross-linked fibrinogen by a dual-enzymatic reaction; were added as a castable ECM [176]. The removal of the fugitive bioink created a formation of connected vascular structure, which supports the enodothelialization and 95% of cell viability was observed.

Liver-on-chip systems attract more attention because of the necessity to improve *in vitro* pre-clinical models, which replicates the human physiology for drug screening. Drug-induced liver injury is the main factor for withdrawing drugs from the market and causes both morbidity and mortality for patients. Also, the success rate of predicting hepatotoxic compounds using animal models is less than 40% due to the human metabolize are different from the most of the other mammals used in the *in vivo* models [177]. Bhise's team developed a liver-on-chip platform by bioprinting hepatic spheroid. In this platform, hepatic spheroids consist of HepG2/C3A cells were incorporated into photocrosslinkable GelMA hydrogel for the assessment of liver toxicity. The system remained functional during the 30 days of culture period, where secretion of albumin and other liver-specific protein and markers were observed. This system was responded similarly to previously reported *in vivo* animal model responses, when 15mM acetaminophen was added as a toxic, indicating the promising tool for assessment of drug toxicity [178].

Lewis lab recently studied the 3D bioprinted human renal proximal tubules on perfusable chips. Perfusion chip gasket was printed using silicone gel mixture, and Fluronic F 127 was used as fugitive ink to make tubular architecture. Gelatin-fibrinogen based gel mixture was used as an ECM material, where thrombin was added to crosslink fibrinogen to form fibrin. These novel 3D proximal tubules on-chip demonstrated significantly enhanced epithelial morphology and functional properties, compared to the 2D controls (with or without perfusion). Furthermore, this model can be used to understand the drug-induced renal damage mechanism [179]. The development of this method provides new routes for kidney-on-chip systems, which could facilitate the advancement of regenerative medicine. 3D printing allows using multiple types of bioink in one system to develop a complex tissue or organ. One such example was done by Parker's team, where they have developed 3D printing methods to utilize six different bioinks with six different purposes to develop a

cardiac device [180]. The development of lab-on-chip devices will provide the capability to overcome the translational challenges associated with animal testing.

5. Future outlook and concluding remarks

3D bioprinting still can be considered as in the early stage of the development, although several tissues at human scale have already successfully created. Currently, the selection of materials for the printing mainly depends on their biocompatibility with cell growth and function and also their printing characteristics, such as viscosity, extrudability, post-printing stability. Therefore, most of the published works use a limited range of bioinks, including alginate, gelatin, collagen, hyaluronic acid, modified copolymer (PEG), and photocurable acrylates/methacrylates. The understanding of the material environment is required to develop a new bioink for 3D bioprinting. One such method is the analyzing composition and distribution of ECM proteins in decellularized tissue scaffolds [9]. The recent advancement in click chemistry and other chemical synthesis processes might be able to develop a functionally adaptive material that reprograms their shape and functionality based on the external stimuli. Although the current 4D bioprinting technique addressed that issue, the current findings are far away from fabricating a successful human-scale tissue construct. The major challenges shared by all researchers in the field of tissue engineering is ensuring sufficient vascularization. The long term cell viability of any bioprinted tissue construct depends on the vascularization. The main challenge is the integrating printed vascular construct into a living host and secondly, replicates the biological functionality and structural complexity of *in vivo* transplant. The 4D bioprinting can be used to fabricate the vascularized model, but the scale-up of those construct into a whole organ is still challenging. The other main paradigm of bioprinting is *in vivo* bioprinting (or *in situ* printing), where the cells and materials directly printed on or in a patient. This approach is already used to bioprint skin directly into a wound and also utilized to bioprint bone into calvaria defects in mice [181]. In conclusion, hydrogel-based bioprinting opens up a new paradigm of tissue engineering and regenerative medicine field. To accomplish success in this rapidly expanding research area, multidisciplinary approach and sustained funding are required.

Acknowledgments

The authors acknowledge funding support from the National Institutes of Health (R01DE023356) and the University ofToledo.

References

[1]. Mandrycky C, Wang Z, Kim K, Kim DH, 3D bioprinting for engineering complex tissues, Biotechnol. Adv. 34 (2016) 422–434, 10.1016/j.biotechadv.2015.12.011. [PubMed: 26724184]

[2]. khademhosseini A, Langer R, Bornestein J, Vacanti JP, Microscale technologies for tissue engineering and biology, Proc. Natl. Acad. Sci. U. S. A. 103 (2006) 2480–2487, 10.1073/pnas.0507681102. [PubMed: 16477028]

[3]. Woodfield TBF, Malda J, De Wijn J, Péters F, Riesle J, Van Blitterswijk CA, Design of porous scaffolds for cartilage tissue engineering using a three-dimensional fiber-deposition technique, Biomaterials 25 (2004) 4149–4161, 10.1016/j.biomaterials.2003.10.056. [PubMed: 15046905]

[4]. Hutmacher DW, Scaffold design and fabrication technologies for engineering tissues - state of the art and future perspectives, J. Biomater. Sci. Polym. Ed. 12 (2001) 107–124, 10.1163/156856201744489. [PubMed: 11334185]

[5]. piard CM, Chen Y, Fisher JP, Cell-laden 3D printed scaffolds for bone tissue engineering, Clin. Rev. Bone Miner. Metab. 13 (2015) 245–255, 10.1007/s12018-015-9198-5.

[6]. Leijten J, Rouwkema J, Zhang YS, Nasajpour A, Dokmeci MR, khademhosseini A, Advancing tissue engineering: a tale of nano-, micro-, and macroscale integration, small 12 (2016) 2130–2145, 10.1002/small.201501798. [PubMed: 27101419]

[7]. Elbert DL, Bottom-up tissue engineering, Curr. Opin. Biotechnol. 22 (2011) 674–680, 10.1016/j.copbio.2011.04.001. [PubMed: 21524904]

[8]. Du Y, Lo E, Ali S, Khademhosseini A, Directed assembly of cell-laden microgels for fabrication of 3D tissue constructs, Proc. Natl. acad. Sci. U. s. A. 105 (2008) 9522–9527, 10.1073/pnas.0801866105. [PubMed: 18599452]

[9]. Murphy SV, Atala A, 3D bioprinting of tissues and organs, Nat. Biotechnol. 32 (2014) 773–785, 10.1038/nbt.2958. [PubMed: 25093879]

[10]. Zhang YS, Yue K, Aleman J, Mollazadeh-Moghaddam K, Bakht SM, Yang J, Jia W, Dell'Erba V, Assawes P, Shin SR, Dokmeci MR, Oklu R, Khademhosseini A, 3D bioprinting for tissue and organ fabrication, Ann. Biomed. Eng. 45 (2017) 148–163, 10.1007/s10439-016-1612-8. [PubMed: 27126775]

[11]. Ashammakhi N, Hasan A, Kaarela O, Byambaa B, Sheikhi A, Gaharwar AK, Khademhosseini A, Advancing frontiers in bone bioprinting, Adv. Healthc. Mater 8 (2019) 1–24, 10.1002/adhm.201801048.

[12]. Ozbolat IT, Hospodiuk M, Current advances and future perspectives in extrusion-based bioprinting, Biomaterials. 76 (2016) 321–343, 10.1016/j.biomaterials.2015.10.076. [PubMed: 26561931]

[13]. Ozbolat IT, Bioprinting scale-up tissue and organ constructs for transplantation, Trends Biotechnol. 33 (2015) 395–400, 10.1016/j.tibtech.2015.04.005. [PubMed: 25978871]

[14]. Guillemot F, Souquet A, Catros S, Guillotin B, Lopez J, Faucon M, Pippenger B, High-throughput laser printing of cells and biomaterials for tissue engineering q, Acta Biomater. 6 (2010) 2494–2500, 10.1016/j.actbio.2009.09.029. [PubMed: 19819356]

[15]. Kim JD, Choi JS, Kim BS, Choi YC, Cho YW, Piezoelectric inkjet printing of polymers: stem cell patterning onpolymer substrates,Polymer (Guildf.) 51 (2010) 2147–2154, 10.1016/j.polymer.2010.03.038.

[16]. Chang CC, Boland ED, Williams SK, Hoying JB, Review direct-write bioprinting three-dimensional biohybrid systems for future regenerative therapies, J. Biomed. Mater. Res. -Part B Appl. Biomater. 98 (2011) 160–170, 10.1002/jbm.b.31831. [PubMed: 21504055]

[17]. Derakhshanfar S, Mbeleck R, Xu K, Zhang X, Zhong W, Xing M, 3D bioprinting for biomedical devices and tissue engineering: a review of recent trends and advances, Bioact. Mater. 3 (2018) 144–156, 10.1016/j.bioactmat.2017.11.008. [PubMed: 29744452]

[18]. Mondschein RJ, Kanitkar A, Williams CB, Verbridge SS, Long TE, Biomaterials Polymer structure-property requirements for stereolithographic 3D printing of soft tissue engineering scaffolds, Biomaterials 140 (2017) 170–188, 10.1016/j.biomaterials.2017.06.005. [PubMed: 28651145]

[19]. Jones N, Three-dimensional printers are opening up new worlds to research, Nature 487 (2012) 22–23. [PubMed: 22763531]

[20]. Dai X, Liu L, Ouyang J, Li X, Zhang X, Lan Q, Xu T, Coaxial 3D bioprinting of self-assembled multicellular heterogeneous tumor fibers, Sci. Rep. (2017) 1–12, 10.1038/s41598-017-01581-y. [PubMed: 28127051]

[21]. Hospodiuk M, Dey M, Sosnoski D, Ozbolat IT, The bioink: a comprehensive review on bioprintable materials, Biotechnol. Adv. 35 (2017) 217–239, 10.1016/j.biotechadv.2016.12.006. [PubMed: 28057483]

[22]. Guillotin B, Guillemot F, Cell patterning technologies for organotypic tissue fabrication, Trends Biotechnol. 29 (2011) 183–190, 10.1016/j.tibtech.2010.12.008. [PubMed: 21256609]

[23]. Norotte C, Marga FS, Niklason LE, Forgacs G, Scaffold-free vascular tissue engineering using bioprinting, Biomaterials 30 (2009) 5910–5917, 10.1016/j.biomaterials.2009.06.034. [PubMed: 19664819]

[24]. Blaeser A, Duarte Campos DF, Fischer H, 3D bioprinting of cell-laden hydrogels for advanced tissue engineering, Curr. Opin. Biomed.Eng. 2 (2017) 58–66, 10.1016/j.cobme.2017.04.003.

[25]. Seol YJ, Kang HW, Lee SJ, Atala A, Yoo JJ, Bioprinting technology and its applications, Eur. J. Cardio-Thoracic Surg. 46 (2014) 342–348, 10.1093/ejcts/ezu148.

[26]. Dababneh AB, Ozbolat IT, Bioprinting technology: a current state-of-the-art review, J. Manuf. Sci. Eng. 136 (2014) 61016, 10.1115/1.4028512.

[27]. Seyednejad H, Gawlitta D, Kuiper RV, DeBruin A, Van Nostrum CF,ingVermonden T, Dhert WJA, Hennink WE, In vivo biocompatibility and biodegradation of 3D-printed porous scsffolds based on a hydroxyl-functionalized poly(ε-caprolactone), Biomaterials 33 (2012) 4309–4318, http://dx.doi.org/l0.1016/j.biomaterials.2012.03.002. [PubMed: 22436798]

[28]. Park SA, Lee SH, Kim WD, Fabrication of porous polycaprolactone/hydroxyapatite (PCL/HA) blend scaffolds using a 3D plotting system for bone tissue engineering, Bioprocess Biosyst. Eng. 34 (2011) 505–513, 10.1007/s00449-010-0499-2. [PubMed: 21170553]

[29]. Pati F, Song TH, Rijal G, Jang J, Kim SW, Cho DW, Ornamenting 3D printed scaffolds with cell-laid extracellular matrix for bone tissue regeneration, Biomaterials 37 (2015) 230–241, 10.1016/j.biomaterials.2014.10.012. [PubMed: 25453953]

[30]. Serra T, Planell JA, Navarro M, High-resolution PLA-based composite scaffolds via 3-D printing technology, Acta Biomater. 9 (2013) 5521–5530, 10.1016/j.actbio.2012.10.041. [PubMed: 23142224]

[31]. Senatov FS, Niaza KV, Zadorozhnyy MY, Maksimkin AV, Kaloshkin SD, Estrin YZ, Mechanical properties and shape memory effect of 3D-printed PLA-based porous scaffolds, J. Mech. Behav. Biomed. Mater. 57 (2016) 139–148, 10.1016/j.jmbbm.2015.11.036. [PubMed: 26710259]

[32]. Almeida CR, Serra T, Oliveira MI, Planell JA, Barbosa MA, Navarro M, Impact of 3-D printed PLA- and chitosan-based scaffolds on human monocyte/macrophage responses: unraveling the effect of 3-D structures on inflammation, Acta Biomater. 10 (2014) 613–622, 10.1016/j.actbio.2013.10.035. [PubMed: 24211731]

[33]. Kao CT, Lin CC, Chen YW, Yeh CH, Fang HY, Shie MY, Poly(dopamine) coating of 3D printed poly(lactic acid) scaffolds for bone tissue engineering, Mater. Sci. Eng. C 56 (2015) 165–173, 10.1016/j.msec.2015.06.028.

[34]. Ge Z, Tian X, Heng BC, Fan V, Yeo JF, Cao T, Histological evaluation of osteogenesis of 3D-printed poly-lactic-co- glycolic acid (PLGA) scaffolds in a rabbit model, Biomed. Mater. 4 (2009) 6–13, 10.1088/1748-6041/4/2/021001.

[35]. Chia HN, Wu BM, High-resolution direct 3D printed PLGA scaffolds: print and shrink, Biofabrication 7 (2015) 15002, 10.1088/17585090/7/1/015002.

[36]. Ge Z, Wang L, Heng BC, Tian XF, Lu K, Fan VTW, Yeo JF, Cao T, Tan E, Proliferation and differentiation of human osteoblasts within 3D printed poly-lactic-co-glycolic acid scaffolds, J. Biomater. Appl. 23 (2009) 533–547, 10.1177/0885328208094301. [PubMed: 18757495]

[37]. Gonçalves EM, Oliveira FJ, Silva RF, Neto MA, Fernandes MH, Amaral M, Vallet-Regí M, Vila M, Three-dimensional printed PCL-hydroxyapatite scaffolds filled with CNTs for bone cell growth stimulation, J. Biomed. Mater. Res. B. Appl. Biomater. 104 (2016) 1210–1219, 10.1002/jbm.b.33432. [PubMed: 26089195]

[38]. Unagolla JM, Jayasuriya AC, Enhanced cell functions on graphene oxide incorporated 3D printed polycaprolactone scaffolds, Mater. Sci. Eng. C 102 (2019) 1–11, 10.1016/j.msec.2019.04.026.

[39]. Won JY, Park CY, Bae JH, Ahn G, Kim C, Lim DH, Cho DW, Yun WS, Shim JH, Huh JB, Evaluation of 3D printed PCL/PLGA/β-TCP versus collagen membranes for guided bone regeneration in a beagle implant model, Biomed. Mater. 11 (2016), 10.1088/1748-6041/11/5/055013.

[40]. Seliktar D, Designing cell-compatible hydrogels for biomedical applications, Science (80-.) 336 (2012) 1124–1128, 10.1126/science.1214804.

[41]. Zhang YS, Khademhosseini A, Advances in engineering hydrogels, Science (80-.) 356 (2017), 10.1126/science.aaf3627.

[42]. Burdick JA, Murphy WL, Moving from static to dynamic complexity in hydrogel design, Nat. Commun. 3 (2012) 1–8, 10.1038/ncomms2271.

[43]. Khetan S, Katz JS, Burdick JA, Sequential crosslinking to control cellular spreading in 3-dimensional hydrogels, Soft Matter 5 (2009) 1601–1606, 10.1039/b820385g.

[44]. Mano F, Reis RL, Gasperini L, Natural polymers for the microencapsulation of cells-revision, J. R. Soc. Interface 11 (2014), 20140817, 10.1098/rsif.2014.0817. [PubMed: 25232055]

[45]. Ward MA, Georgiou TK, Thermoresponsive polymers for biomedical applications, Polymers (Basel) 3 (2011) 1215–1242, 10.3390/polym3031215.

[46]. Klouda L, Mikos AG, Thermoresponsive hydrogels in biomedical applications, Eur. J. Pharm. Biopharm. 68 (2008) 34–45, 10.1016/j.ejpb.2007.02.025. [PubMed: 17881200]

[47]. Glatzel S, Laschewsky A, Lutz JF, Well-defined uncharged polymers with a sharp UCST in water and in physiological milieu, Macromolecules 44 (2011) 413–415, 10.1021/ma102677k.

[48]. Zhang S, Fabrication of novel biomaterials through molecular self-assembly, Nat. Biotechnol. 21 (2003) 1171–1178, 10.1038/nbt874. [PubMed: 14520402]

[49]. Appel EA, Tibbitt MW, Webber MJ, Mattix BA, Veiseh O, Langer R, Self-assembled hydrogels utilizing polymer-nanoparticle interactions, Nat. Commun. 6(2015) 1–9, 10.1038/ncomms7295.

[50]. Loebel C, Rodell CB, Chen MH, Burdick JA, Shear-thinning and self-healing hydrogels as injectable therapeutics and for 3D-printing, Nat. Protoc. 12 (2017) 1521–1541, 10.1038/nprot.2017.053. [PubMed: 28683063]

[51]. Hoffman AS, Hydrogels for biomedical applications, Ann. New York Acad. Sci. (2006) 62–73, 10.1111/j.1749-6632.2001.tb03823.x.

[52]. Rowley JA, Madlambayan G, Mooney DJ, Alginate hydrogels as synthetic extracellular matrix materials, Biomaterials 20 (1999) 45–53, 10.1016/S0142-9612(98)00107-0. [PubMed: 9916770]

[53]. Kuo CK, Ma PX, Ionically crosslinked alginate hydrogels as scaffolds for tissue engineering: part 1. Structure, gelation rate and mechanical properties, Biomaterials 22 (2001) 511–521, 10.1016/S0142-9612(00)00201-5. [PubMed: 11219714]

[54]. Morton SW, Herlihy KP, Shopsowitz KE, Deng ZJ, Chu ICS, Bowerman CJ, Desimone JM, Hammond PT, Scalable manufacture of built-to-order nanomedicine: spray-assisted layer-by-layer functionalization of PRINT nanoparticles, Adv. Mater. 25 (2013) 4707–4713, 10.1002/adma.201302025. [PubMed: 23813892]

[55]. Hennink Wim E., van Nostrum CF, Novel crosslinking methods to design hydrogels, Adv. DrugDeliv. Rev. 54 (2002) 13–36, 10.1016/S0169-409X(01)00240-X.

[56]. DeForest CA, Anseth KS, Cytocompatible click-based hydrogels with dynamically tunable properties through orthogonal photoconjugation and photocleavage reactions, Nat. Chem. 3 (2011) 925–931, 10.1038/nchem.ll74. [PubMed: 22109271]

[57]. Deforest CA, Polizzotti BD, Anseth KS, Sequential click reactions for synthesizing and patterning three-dimensional cell microenvironments, Nat. Mater. 8 (2009) 659–664, 10.1038/nmat2473. [PubMed: 19543279]

[58]. Kharkar PM, Kiick KL, Kloxin AM, Designing degradable hydrogels for orthogonal control of cell microenvironments, Chem. Soc. Rev. 42 (2013) 7335–7372, 10.1039/c3cs60040h. [PubMed: 23609001]

[59]. Azagarsamy MA, Anseth ICS, Bioorthogonal click chemistry: an indispensable tool to create multifaceted cell culture scaffolds, ACS Macro Lett. 2 (2013) 5–9, 10.1021/mz300585q. [PubMed: 23336091]

[60]. Williams DF, On the mechanisms of biocompatibility, Biomaterials 29 (2008) 2941–2953, 10.1016/j.biomaterials.2008.04.023. [PubMed: 18440630]

[61]. Kretlow JD, Mikos AG, From material to tissue: biomaterial development, scaffold fabrication, and tissue engineering, AIChE J. 54 (2008) 3048–3067, 10.1002/aic. [PubMed: 19756176]

[62]. Novosel EC, Kleinhans C, Kluger PJ, Vascularization is the key challenge in tissue engineering, Adv. Drug Deliv. Rev. 63 (2011) 300–311, 10.1016/j.addr.2011.03.004. [PubMed: 21396416]

[63]. Nelson CM, Bissell MJ, Of extracellular matrix, scaffolds, and signaling: tissue architecture regulates development, homeostasis, and cancer, Annu. Rev. Cell Dev. Biol. 22 (2006) 287–309, 10.1146/annurev.cellbio.22.010305.104315. [PubMed: 16824016]

[64]. Berg J, Hiller T, Kissner MS, Qazi TH, Duda GN, Hocke AC, Hippenstiel S, Elomaa L, Weinhart M, Fahrenson C, Kurreck J, Optimization of cell-laden bioinks for 3D bioprinting and efficient infection with influenza A virus, Sci. Rep. 8 (2018) 1–13, 10.1038/s41598-018-31880-x. [PubMed: 29311619]

[65]. Engler AJ, Sen S, Sweeney HL, Discher DE, Matrix elasticity directs stem cell lineage specification, Cell 126 (2006) 677–689, 10.1016/j.cell.2006.06.044. [PubMed: 16923388]

[66]. Discher DE, Janmey P, Wang Y, Tissue cells feel and respond to the stiffness of their substrate, Science (80-.) 310 (2005) 1139–1143, 10.1126/science.1116995.

[67]. Andersen T, Auk-Emblem P, Dornish M, 3D cell culture in alginate hydrogels, Microarrays 4 (2015) 133–161, 10.3390/microarrays4020133. [PubMed: 27600217]

[68]. Axpe E, Oyen ML, Applications of alginate-based bioinks in 3D bioprinting, Int. J. Mol. Sci. 17 (2016), 10.3390/ijms17121976.

[69]. Arne H, Smidsrod O, The effect of divalent metals on the properties of alginate solutions 2. Comparison of different metal ions, Acta Chem. Scand. 19 (1965) 341–351, 10.3891/acta.chem.scand.19-0341.

[70]. Braccini I, Perez S, Molecular basis of Ca2+-induced gelation in alginates and pectins: the egg-box model revisited, Biomacromolecules. 2 (2001) 1089–1096, 10.1021/bm010008g. [PubMed: 11777378]

[71]. Schmidt JJ, Rowley J, Hyun JK, Hydrogels used for cell-based drug delivery, J. Biomed. Mater. Res. - Part A. 87 (2008) 1113–1122, 10.1002/jbm.a.32287.

[72]. Miri AK, Khalilpour A, Cecen B, Maharjan S, Shin SR, Khademhosseini A, Multiscale bioprinting of vascularized models, Biomaterials 198 (2019) 204–216, 10.1016/j.biomaterials.2018.08.006. [PubMed: 30244825]

[73]. Jia J, Richards DJ, Pollard S, Tan Y, Rodriguez J, Visconti RP, Trusk TC, Yost MJ, Yao H, Markwald RR, Mei Y, Engineering alginate as bioink for bioprinting, Acta Biomater. 10 (2014) 4323–4331, 10.1016/j.actbio.2014.06.034. [PubMed: 24998183]

[74]. Freeman FE, Kelly DJ, Tuning alginate bioink stiffness and composition for controlled growth factor delivery and to spatially direct MSC Fate within bioprinted tissues, Sci. Rep. 7 (2017) 1–12, 10.1038/s41598-017-17286-1. [PubMed: 28127051]

[75]. Bouhadir KH, Lee KY, Alsberg E, Damm KL, Anderson KW, Mooney DJ, Degradation of partially oxidized alginate and its potential application for tissue engineering, Biotechnol. Prog. 17 (2001) 945–950, 10.1021/bp010070p. [PubMed: 11587588]

[76]. Colosi C, Shin SR, Manoharan V, Massa S, Costantini M, Barbetta A, Dokmeci MR, Dentini M, Khademhosseini A, Microfluidic bioprinting of heterogeneous 3D tissue constructs using low-viscosity bioink, Adv. Mater. 28 (2016) 677–684, 10.1002/adma.201503310. [PubMed: 26606883]

[77]. Gao Q, He Y, Fu J. zhong, Liu A, Ma L, Coaxial nozzle-assisted 3D bioprinting with built-in microchannels for nutrients delivery, Biomaterials 61 (2015) 203–215, 10.1016/j.biomaterials.2015.05.031. [PubMed: 26004235]

[78]. Tabriz AG, Hermida MA, Leslie NR, Shu W, Three-dimensional bioprinting of complex cell laden alginate hydrogel structures three-dimensional bioprinting of complex cell laden alginate hydrogel structures, Biofabrication 7 (2015), 45012 http://stacks.iop.org/1758-5090/7/i=4/a=045012.

[79]. Zhang Y, Yu Y, Chen H, Ozbolat IT, Characterization of printable cellular micro-fluidic channels for tissue engineering, Biofabrication 5 (2013), 10.1088/1758-5082/5/2/025004.

[80]. Yu Y, Zhang Y, Martin JA, Ozbolat IT, Evaluation of cell viability and functionality in vessel-like bioprintable cell-laden tubular channels, J. Biomech. Eng. 135 (2013) 91011, 10.1115/l.4024575. [PubMed: 23719889]

[81]. Attalla R, ling C, Selvaganapathy P, Fabrication and characterization of gels with integrated channels using 3D printing with microfluidic nozzle for tissue engineering applications, Biomed. Microdevices 18 (2016) 1–12, 10.1007/s10544-016-0042-6. [PubMed: 26660457]

[82]. Mistry P, Aied A, Alexander M, Shakesheff K, Bennett A, Yang J, Bioprinting using mechanically robust core-shell cell-laden hydrogel strands, Macromol. Biosci. 17 (2017) 1–8, 10.1002/mabi.201600472.

[83]. Markstedt K, Mantas A, Tournier I, Ha D, Gatenholm P, 3D bioprinting human chondrocytes with nanocellulose - alginate bioink for cartilage tissue engineering applications, Biomacromolecules 16 (2015) 1489–1496, 10.1021/acs.biomac.5b00188. [PubMed: 25806996]

[84]. Li H, Tan YJ, Leong KF, Li L, 3D bioprinting of highly thixotropic alginate/methylcellulose hydrogel with strong interface bonding, ACS Appl. Mater. Interfaces 9 (2017) 20086–20097, 10.1021/acsami.7b04216. [PubMed: 28530091]

[85]. Wiist S, Godla ME, Müller R, Hofmann S, Tunable hydrogel composite with two-step processing in combination with innovative hardware upgrade for cell-based three-dimensional bioprinting, Acta Biomater. 10 (2014) 630–640, 10.1016/j.actbio.2013.10.016. [PubMed: 24157694]

[86]. Feng Q, Neufurth M, Wang X, Schr HC, Ziebart T, Steffen R, Wang S, Muller WEG, Engineering a morphogenetically active hydrogel for bioprinting of bioarti fi cial tissue derived from human osteoblast-like SaOS-2 cells, Biomaterials 35 (2014) 8810–8819, 10.1016/j.biomaterials.2014.07.002. [PubMed: 25047630]

[87]. Bendtsen ST, Quinnell SP, Wei M, Development of a novel alginate-polyvinyl alcohol-hydroxyapatite hydrogel for 3D bioprinting bone tissue engineered scaffolds, J. Biomed. Mater. Res. - Part A 105 (2017) 1457–1468, 10.1002/jbm.a36036.

[88]. Lee H, Ahn S, Bonassar LJ, Kim G, Cell(MC3T3-E1)-printed poly(−caprolactone)/ɛ alginate hybrid scaffolds for tissue regeneration, Macromol. Rapid Commun. 34 (2013) 142–149. [PubMed: 23059986]

[89]. Kundu J,Shim J-H, Jang J, Kim S-W, Cho D-W, An additive manufacturing-based PCL-alginate-chondrocyte bioprinted scaffold for cartilage tissue engineering,J. Tissue Eng. Re gen. Med. 9 (2015) 1286–1297, 10.1002/term.1682.

[90]. Poldervaart MT, Wang H, Van Der Stok J, Weinans H, Leeuwenburgh SCG, Oner FC, Dhert WJA, Alblas J, Sustained release of BMP-2 in bioprinted alginate for osteogenicity in mice and rats, PLoS One 8 (2013), e72610, 10.1371/journal.pone.0072610. [PubMed: 23977328]

[91]. Wang Q,, Xia Q, Wu Y, Zhang X, Wen F, Chen X, Zhang S, Heng BC, He Y, Ouyang HW, 3D-printed atsttrin-incorporated alginate/hydroxyapatite scaffold promotes bone defect regeneration with TNF/TNFR signaling involvement, Adv. Healthc. Mater. 4 (2015) 1701–1708, 10.1002/adhm.201500211. [PubMed: 26085382]

[92]. Parenteau-Bareil R, Gauvin R, Berthod F, Collagen-based biomaterials for tissue engineering applications, Materials (Basel) 3 (2010) 1863–1887, 10.3390/ma3031863.

[93]. Xing R, Liu K, Jiao T, Zhang N, Ma K, Zhang R, Zou Q, Ma G, Yan X, An injectable self-assembling collagen-gold hybrid hydrogel for combinatorial antitumor photothermal/photodynamic therapy, Adv. Mater. 28 (2016) 3669–3676, 10.1002/adma.201600284. [PubMed: 26991248]

[94]. Park JY, Choi JC, Shim JH, Lee JS, Park H, Kim SW, Doh J, Cho DW, A comparative study on collagen type i and hyaluronic acid dependent cell behavior for osteochondral tissue bioprinting, Biofabrication 6 (2014), 10.1088/1758-5082/6/3/035004.

[95]. Yeo MG, Lee JS, Chun W, Kim GH, An innovative collagen-based cell-printing method for obtaining human adipose stem cell-laden structures consisting of core-sheath structures for tissue engineering, Biomacromolecules 17 (2016) 1365–1375, 10.1021/acs.biomac.5b01764. [PubMed: 26998966]

[96]. Rhee S, Puetzer JL, Mason BN, Reinhart-King CA, Bonassar LJ, 3D bioprinting of spatially heterogeneous collagen constructs for cartilage tissue engineering, ACS Biomater. Sci. Eng. 2 (2016) 1800–1805, 10.1021/acsbiomaterials.6b00288.

[97]. Nicole D, Louis W, Tylar P, Joseph S, Caroline D, Sonya S, Stephen K, Lawrence JB, Correlating rheological properties and printability of collagen bioinks: the effects of riboflavin photocrosslinking and pH, Biofabrication 9 (2017), 34102 http://stacks.iop.org/1758-5090/9/i=3/a=034102.

[98]. Ibusuki S, Halbesma GJ, Randolph MA, Redmond RW, Kochevar IE, Gill TJ, Photochemically cross-linked collagen gels as three-dimensional scaffolds for tissue engineering, Tissue Eng. 13 (2007) 1995–2001, 10.1089/ten.2006.0153. [PubMed: 17518705]

[99]. Skardal A, Mack D, Kapetanovic E, Atala A, Jackson JD, Yoo J, Soker S, Bioprinted amniotic fluid-derived stem cells accelerate healing of large skin wounds, Stem Cells Transl. Med. 1 (2012) 792–802, 10.5966/sctm.2012-0088. [PubMed: 23197691]

[100]. Yanez M, Rincon J, Dones A, De Maria C, Gonzales R, Boland T, In vivo assessment of printed microvasculature in a bilayer skin graft to treat full-thickness wounds, Tissue Eng. Part A 21 (2014) 224–233, 10.1089/ten.tea.2013.0561. [PubMed: 25051339]

[101]. Michael S, Sorg H, Peck CT, Koch L, Deiwick A, Chichkov B, Vogt PM, Reimers K, Tissue engineered skin substitutes created by laser-assisted bioprinting form skin-like structures in the dorsal skin fold chamber in mice, PLoS One 8 (2013), 10.1371/journal.pone.0057741.

[102]. Yang X, Lu Z, Wu H, Li W, Zheng L, Zhao J, Collagen-alginate as bioink for three-dimensional (3D) cell printing based cartilage tissue engineering, Mater. Sci. Eng. C 83 (2018) 195–201, 10.1016/j.msec.2017.09.002.

[103]. Ng WL, Goh MH, Yeong WY, Naing MW, Applying macromolecular crowding to 3D bioprinting: fabrication of 3D hierarchical porous collagen-based hydrogel constructs, Biomater. Sci. 6 (2018) 562–574, 10.1039/c7bm01015j. [PubMed: 29383354]

[104]. Levengood SKL, Zhang M, Chitosan-based scaffolds for bone tissue engineering,J. Mater. Chem. B 2 (2014) 3161–3184, 10.1039/c4tb00027g. [PubMed: 24999429]

[105]. Unagolla JM, Alahmadi TE, Jayasuriya AC, Chitosan microparticles based polyelectrolyte complex scaffolds for bone tissue engineering in vitro and effect of calcium phosphate, Carbohydr. Polym. 199 (2018) 426–436, 10.1016/j.carbpol.2018.07.044. [PubMed: 30143148]

[106]. Seda Tiğli R, Karakepli A, Gumusderelioglu M, In vitro characterization of chitosan scaffolds: influence of composition and deacetylation degree, J. Mater. Sci. Mater. Med. 18 (2007) 1665–1674, 10.1007/S10856-007-3066-X. [PubMed: 17483879]

[107]. Dong L, Wang SJ, Zhao XR, Zhu YF, Yu JK, 3D-printed poly (e-caprolactone) scaffold integrated with cell-laden chitosan hydrogels for bone tissue engineering, Sci. Rep. 7 (2017) 4–12, 10.1038/s41598-017-13838-7. [PubMed: 28127054]

[108]. Bruzvau skait_e I, Bironait D, Bagdonas E, Bernotien_e E, Scaffolds and cells for tissue regeneration: different scaffold pore sizes — different cell effects, Cytotechnology 68 (2016) 355–369, 10.1007/sl0616-0159895-4. [PubMed: 26091616]

[109]. Huang J, Fu H, Wang Z, Meng Q,, Liu S, Wang H, Zheng X, Dai J, Zhang Z, BMSCs-laden gelatin/sodium alginate/carboxymethyl chitosan hydrogel for 3D bioprinting, RSC Adv. 6(2016) 108423–108430, 10.1039/c6ra24231f.

[110]. Prestwich GD, Hyaluronic acid-based clinical biomaterials derived for cell and molecule delivery in regenerative medicine, J. Control. Release 155 (2011) 193–199, 10.1016/j.jconrel.2011.04.007. [PubMed: 21513749]

[111]. Gaetani R, Feyen DAM, Verhage V, Slaats R, Messina E, Christman KL, Giacomello A, Doevendans PAFM, Sluijter JPG, Epicardial application of cardiac progenitor cells in a 3D-printed gelatin/hyaluronic acid patch preserves cardiac function after myocardial infarction, Biomaterials 61 (2015) 339–348, 10.1016/j.biomaterials.2015.05.005. [PubMed: 26043062]

[112]. Law N, Doney B, Glover H, Qin Y, Aman ZM, Sercombe TB, Liew LJ, Dilley RJ, Doyle BJ, Characterisation of hyaluronic acid methylcellulose hydrogels for 3D bioprinting, J. Mech. Behav. Biomed. Mater. 77 (2018) 389–399, 10.1016/jjmbbm.2017.09.031. [PubMed: 29017117]

[113]. Rajaram A, Schreyer DJ, Chen DXB, Use of the polycation polyethyleneimine to improve the physical properties of alginate-hyaluronic acid hydrogel during fabrication of tissue repair scaffolds, J. Biomater. Sci. Polym. Ed. 26 (2015) 433–445, 10.1080/09205063.2015.1016383. [PubMed: 25661399]

[114]. Ouyang L, Highley CB, Rodell CB, Sun W, Burdick JA, 3D printing of shear-thinning hyaluronic acid hydrogels with secondary cross-linking, ACS Biomater. Sci. Eng. 2 (2016) 1743–1751, 10.1021/acsbiomaterials.6b00158.

[115]. Raucci MG, D'Amora U, Ronca A, Demitri C, Ambrosio L, Bioactivation routes of gelatin-based scaffolds to enhance at nanoscale level bone tissue regeneration, Front. Bioeng. Biotechnol. 7 (2019) 1–11, 10.3389/fbioe.2019.00027. [PubMed: 30705882]

[116]. Choi DJ, Park SJ, Gu BK, Kim YJ, Chung S, Kim CH, Effect of the pore size in a 3D bioprinted gelatin scaffold on fibroblast proliferation, J. Ind. Eng. Chem. 67 (2018) 388–395, 10.1016/jjiec.2018.07.013.

[117]. Laronda MM, Rutz AL, Xiao S, Whelan ICA, Duncan FE, Roth EW, Woodruff TK, Shah RN, A bioprosthetic ovary created using 3D printed microporous scaffolds restores ovarian function in sterilized mice, Nat. Commun. 8 (2017) 1–10, 10.1038/ncommsl5261. [PubMed: 28232747]

[118]. Duan B, Hockaday LA, Kang KH, Butcher JT, 3D Bioprinting of heterogeneous aortic valve conduits with alginate/gelatin hydrogels, J. Biomed. Mater. Res. - Part A 101 (2013) 1255–1264, 10.1002/jbm.a.34420.

[119]. Di Giuseppe M, Law N, Webb B, Macrae RA, Liew LJ, Sercombe TB, Dilley RJ, Doyle BJ, Mechanical behaviour of alginate-gelatin hydrogels for 3D bioprinting, J. Mech. Behav. Biomed. Mater. 79 (2018) 150–157, 10.1016/j.jmbbm.2017.12.018. [PubMed: 29304429]

[120]. Rutz AL, Hyland KE, Jakus AE, Burghardt WR, Shah RN, A multimaterial bioink method for 3D printing tunable, cell-compatible hydrogels, Adv. Mater. 27 (2015) 1607–1614, 10.1002/adma.201405076. [PubMed: 25641220]

[121]. Kang HW, Lee SJ, Ko IK, Kengla C, Yoo JJ, Atala A, A 3D bioprinting system to produce human-scale tissue constructs with structural integrity, Nat. Biotechnol. 34 (2016) 312–319, 10.1038/nbt.3413. [PubMed: 26878319]

[122]. Skardal A, Devarasetty M, Kang HW, Mead I, Bishop C, Shupe T, Lee SJ, Jackson J, Yoo J, Soker S, Atala A, A hydrogel bioink toolkit for mimicking native tissue biochemical and mechanical properties in bioprinted tissue constructs, Acta Biomater. 25 (2015) 24–34, 10.1016/j.actbio.2015.07.030. [PubMed: 26210285]

[123]. Van Den Bulcke AI, Bogdanov B, De Rooze N, Schacht EH, Cornelissen M, Berghmans H, Structural and rheological properties of methacrylamide modified gelatin hydrogels, Biomacromolecules 1 (2000) 31–38, 10.1021/bm990017d. [PubMed: 11709840]

[124]. Klotz BJ, Gawlitta D, Rosenberg AJWP, Malda J, Melchels FPW, Gelatin-methacryloyl hydrogels: towards biofabrication-based tissue repair, Trends Biotechnol. 34 (2016) 394–407, 10.1016/j.tibtech.2016.01.002. [PubMed: 26867787]

[125]. Nguyen KT, West JL, Photopolymerizable hydrogels for tissue engineering applications, Biomaterials 23 (2002) 4307–4314, 10.1016/S0142-9612(02)00175-8. [PubMed: 12219820]

[126]. Nguyen AH, McKinney J, Miller T, Bongiorno T, McDevitt TC, Gelatin methacrylate microspheres for controlled growth factor release, Acta Biomater. 13 (2015) 101–110, 10.1016/j.actbio.2014.11.028. [PubMed: 25463489]

[127]. Bertassoni LE, Cardoso JC, Manoharan V, Cristino AL, Bhise NS, Araujo WA, Zorlutuna P, Vrana NE, Ghaemmaghami AM, Dokmeci MR, Khademhosseini A, Direct-write bioprinting of cell-laden methacrylated gelatin hydrogels, Biofabrication 6 (2014), 10.1088/17585082/6/2/024105.

[128]. Nichol JW, Koshy ST, Bae H, Hwang CM, Yamanlar S, Khademhosseini A, Cell-laden microengineered gelatin methacrylate hydrogels, Biomaterials 31 (2010) 5536–5544, 10.1016/j.biomaterials.2010.03.064. [PubMed: 20417964]

[129]. Chen YC, Lin RZ, Qi H, Yang Y, Bae H, Melero-Martin JM, Khademhosseini A, Functional human vascular network generated in photocrosslinkable gelatin methacrylate hydrogels, Adv. Funct. Mater. 22 (2012) 2027–2039, 10.1002/adfm.201101662. [PubMed: 22907987]

[130]. Liu W, Heinrich MA, Zhou Y, Akpek A, Hu N, Liu X, Guan X, Zhong Z, Jin X, Khademhosseini A, Zhang YS, Extrusion bioprinting of shear-thinning gelatin methacryloyl bioinks, Adv. Healthc. Mater. 6 (2017) 1–11, 10.1002/adhm.201601451.

[131]. Zhang YS, Arneri A, Bersini S, Shin SR, Zhu K, Goli-Malekabadi Z, Aleman J, Colosi C, Busignani F, Dell'Erba V, Bishop C, Shupe T, Demarchi D, Moretti M, Rasponi M, Dokmeci MR, Atala A, Khademhosseini A, Bioprinting 3D microfibrous scaffolds for engineering endothelialized myocardium and heart-on-a-chip, Biomaterials 110 (2016) 45–59, 10.1016/j.biomaterials.2016.09.003. [PubMed: 27710832]

[132]. Billiet T, Gevaert E, De Schryver T, Cornelissen M, Dubruel P, The 3D printing of gelatin methacrylamide cell-laden tissue-engineered constructs with high cell viability, Biomaterials 35 (2014) 49–62, 10.1016/j.biomaterials.2013.09.078. [PubMed: 24112804]

[133]. Wang Z, Jin X, Dai R, Holzman JF, Kim K, An ultrafast hydrogel photocrosslinking method for direct laser bioprinting, RSC Adv. 6 (2016) 21099–21104, 10.1039/c5ra24910d.

[134]. Ma X, Qu X, Zhu W, Li Y, Yuan S, Zhang H, Liu J, Wang P, Laic CSE, Zanellae F, Feng G-S, Sheikhe F, Chien S, Chen S, Deterministically patterned biomimetic human iPSC- derived hepatic model via rapid 3D bioprinting, Proc. Natl. Acad. Sci. U. S. A. 113 (2016) 2206–2211, 10.1073/pnas.1524510113. [PubMed: 26858399]

[135]. Yin J, Yan M, Wang Y, Fu J, Suo H, 3D bioprinting of low-concentration cell-laden gelatin methacrylate (GelMA) bioinks with a two-step cross-linking strategy, ACS Appl. Mater. Interfaces 10 (2018) 6849–6857, 10.1021/acsami.7b16059. [PubMed: 29405059]

[136]. Visser J, Melchels FPW, Jeon JE, van Bussel EM, Kimpton LS, Byrne HM, Dhert WJA, Dalton PD, Hutmacher DW, Malda J, Reinforcement of hydrogels using three-dimensionally printed microfibres, Nat. Commun. 6 (2015) 6933, 10.1038/ncomms7933. [PubMed: 25917746]

[137]. Schuurman W, Levett PA, Pot MW, van Weeren PR, Dhert WJA, Hutmacher DW, Melchels FPW, Klein TJ, Malda J, Gelatin-methacrylamide hydrogels as potential biomaterials for fabrication of tissue-engineered cartilage constructs, Macromol. Biosci. 13 (2013) 551–561, 10.1002/mabi.201200471. [PubMed: 23420700]

[138]. Zustiak SP, Leach JB, Hydrolytically degradable poly(ethylene glycol) hydrogel scaffolds with tunable degradation and mechanical properties, Biomacromolecules 11 (2010) 1348–1357, 10.1021/bm100137q. [PubMed: 20355705]

[139]. Peppas NA, Keys KB, Torres-Lugo M, Lowman AM, Poly(ethylene glycol)-containing hydrogels in drug delivery, J. Control. Release 62 (1999) 81–87, http://dx.doi.org/l0.1016/S0168-3659(99)00027-9. [PubMed: 10518639]

[140]. Zhu J, Bioactive modification of poly(ethylene glycol) hydrogels for tissue engineering, Biomaterials 31 (2010) 4639–4656, 10.1016/j.biomaterials.2010.02.044. [PubMed: 20303169]

[141]. Skardal A, Zhang J, Prestwich GD, Bioprinting vessel-like constructs using hyaluronan hydrogels crosslinked with tetrahedral polyethylene glycol tetracrylates, Biomaterials 31 (2010) 6173–6181, 10.1016/j.biomaterials.2010.04.045. [PubMed: 20546891]

[142]. Jia W, Gungor-Ozkerim PS, Zhang YS, Yue K, Zhu K, Liu W, Pi Q,, Byambaa B, Dokmeci MR, Shin SR, Khademhosseini A, Direct 3D bioprinting of perfusable vascular constructs using a blend bioink, Biomaterials 106 (2016) 58–68, 10.1016/j.biomaterials.2016.07.038. [PubMed: 27552316]

[143]. Bertassoni LE, Cecconi M, Manoharan V, Nikkhah M, Hjortnaes J, Cristino AL, Barabaschi G, Demarchi D, Dokmeci MR, Yang Y, Khademhosseini A, Hydrogel bioprinted microchannel networks for vascularization of tissue engineering constructs, Lab Chip 14 (2014) 2202–2211, 10.1039/c41c00030g. [PubMed: 24860845]

[144]. Wang Z, Abdulla R, Parker B, Samanipour R, Ghosh S, Kim K, A simple and high-resolution stereolithography-based 3D bioprinting system using visible light crosslinkable bioinks, Biofabrication 7 (2015)45009, 10.1088/1758-5090/7/4/045009.

[145]. Gao G, Schilling AF, Yonezawa T, Wang J, Dai G, Cui X, Bioactive nanoparticles stimulate bone tissue formation in bioprinted three-dimensional scaffold and human mesenchymal stem cells, Biotechnol. J 9 (2014) 1304–1311, 10.1002/biot.201400305. [PubMed: 25130390]

[146]. Gao G, Yonezawa T, Hubbell K, Dai G, Cui X, Inkjet-bioprinted acrylated peptides and PEG hydrogel with human mesenchymal stem cells promote robust bone and cartilage formation with minimal printhead clogging, Biotechnol. J. 10(2015) 1568–1577, 10.1002/biot.201400635. [PubMed: 25641582]

[147]. Gao G, Schilling AF, Hubbell K, Yonezawa T, Truong D, Hong Y, Dai G, Cui X, Improved properties of bone and cartilage tissue from 3D inkjet-bioprinted human mesenchymal stem cells by simultaneous deposition and photocrosslinking in PEG-GelMA, Biotechnol. Lett. 37 (2015) 2349–2355, 10.1007/sl0529-015-1921-2. [PubMed: 26198849]

[148]. Zheng Z, Wu J, Liu M, Wang H, Li C, Rodriguez MJ, Li G, Wang X, Kaplan DL, 3D bioprinting of self-standing silk-based bioink, Adv. Healthc. Mater. 7 (2018) 1–12, 10.1002/adhm.201701026.

[149]. Xin S, Chimene D, Garza JE, Gaharwar AK, Alge DL, Clickable PEG hydrogel microspheres as building blocks for 3D bioprinting, Biomater. Sci. 7 (2019) 1179–1187, 10.1039/c8bm01286e. [PubMed: 30656307]

[150]. Daniele MA, Adams AA, Naciri J, North SH, Ligler FS, Interpenetrating networks based on gelatin methacrylamide and PEG formed using concurrent thiol click chemistries for hydrogel tissue engineering scaffolds, Biomaterials 35 (2014) 1845–1856, 10.1016/j.biomaterials.2013.11.009. [PubMed: 24314597]

[151]. Tan Y, Richards DJ, Trusk TC, Visconti RP, Yost MJ, Kindy MS, Drake CJ, Argraves WS, Markwald RR, Mei Y, 3D printing facilitated scaffold-free tissue unit fabrication, Biofabrication 6 (2014), 10.1088/1758-5082/6/2/024111.

[152]. Stevens KR, Bendixen K, Regnier M, Dupras SK, Muskheli V, Kreutziger KL, Reinecke H, Nourse MB, Korte FS, Murry CE, Physiological function and transplantation of scaffold-free and vascularized human cardiac muscle tissue, Proc. Natl. Acad. Sci. U. S. A. 106 (2009) 16568–16573, 10.1073/pnas.0908381106. [PubMed: 19805339]

[153]. Takebe T, Sekine K, Enomura M, Koike H, Kimura M, Ogaeri T, Zhang RR, Ueno Y, Zheng YW, Koike N, Aoyama S, Adachi Y, Taniguchi H, Vascularized and functional human liver from an iPSC-derived organ bud transplant, Nature 499 (2013) 481–484, 10.1038/nature12271. [PubMed: 23823721]

[154]. Xu C, Chai W, Huang Y, Markwald RR, Scaffold-free inkjet printing of three-dimensional zigzag cellular tubes, Biotechnol. Bioeng. 109 (2012) 3152–3160, 10.1002/bit.24591. [PubMed: 22767299]

[155]. Yu Y, Moncal KK, Li J, Peng W, Rivero I, Martin JA, Ozbolat IT, Three-dimensional bioprinting using self-Assembling scalable scaffold-free “tissue strands” as a new bioink, Sci. Rep. 6 (2016) 1–11, 10.1038/srep28714. [PubMed: 28442746]

[156]. Gruene M, Deiwick A, Koch L, Schlie S, Unger C, Hofmann N, Bernemann I, Glasmacher B, Chichkov B, Laser printing of stem cells for biofabrication of scaffold-free autologous grafts, Tissue Eng. Part C Methods 17 (2011) 79–87, 10.1089/ten.tec.2010.0359. [PubMed: 20673023]

[157]. Sydney Gladman A, Matsumoto EA, Nuzzo RG, Mahadevan L, Lewis JA, Biomimetic 4D printing, Nat. Mater. 15 (2016) 413–418, 10.1038/nmat4544. [PubMed: 26808461]

[158]. Deforest CA, Tirrell DA, A photoreversible protein-patterning approach for guiding stem cell fate in three-dimensional gels, Nat. Mater. 14 (2015) 523–531, 10.1038/nmat4219. [PubMed: 25707020]

[159]. Wang T, Zheng S, Sun W, Liu X, Fu S, Tong Z, Notch insensitive and self-healing PNIPAm-PAM-clay nanocomposite hydrogels, Soft Matter 10 (2014) 3506–3512, 10.1039/c3sm52961d. [PubMed: 24652073]

[160]. Villar G, Heron AJ, Bayley H, Formation of droplet networks that function in aqueous environments, Nat. Nanotechnol. 6 (2011) 803–808, 10.1038/nnano.2011.183. [PubMed: 22056724]

[161]. Kokkinis D, Schaffner M, Studart AR, Multimaterial magnetically assisted 3D printing of composite materials, Nat. Commun. 6 (2015) 8643, 10.1038/ncomms9643. [PubMed: 26494528]

[162]. Dvir T, Timko BP, Kohane DS, Langer R, Nanotechnological strategies for engineering complex tissues, Nat. Nanotechnol. 6 (2011) 13–22, 10.1038/nnano.2010.246. [PubMed: 21151110]

[163]. Khoo ZX, Teoh JEM, Liu Y, Chua CK, Yang S, An J, Leong KF, Yeong WY, 3D printing of smart materials: a review on recent progresses in 4D printing, Virtual Phys. Prototyp. 10(2015) 103–122, 10.1080/17452759.2015.1097054.

[164]. Bakarich SE, Gorkin R, In Het Panhuis M, Spinks GM, 4D printing with mechanically robust, thermally actuating hydrogels, Macromol. Rapid Commun. 36 (2015) 1211–1217, 10.1002/marc.201500079. [PubMed: 25864515]

[165]. Guo J, Zhang R, Zhang L, Cao X, 4D printing of robust hydrogels consisted of agarose nanofibers and polyacrylamide, ACS Macro Lett. 7 (2018) 442–446, 10.1021/acsmacrolett.7b00957.

[166]. Jamal M, Kadam SS, Xiao R, Jivan F, Onn TM, Fernandes R, Nguyen TD, Gracias DH, Bio-origami hydrogel scaffolds composed of photocrosslinked PEG bilayers, Adv. Healthc. Mater. 2 (2013) 1142–1150, 10.1002/adhm.201200458. [PubMed: 23386382]

[167]. Kirillova A, Maxson R, Stoychev G, Gomillion CT, Ionov L, 4D biofabrication using shape-morphing hydrogels, Adv. Mater. 29 (2017) 1–8, 10.1002/adma.201703443.

[168]. Shin SR, Migliori B, Miccoli B, Li Y, Mostafalu P, Seo J, Mandla S, Enrico A, Antona S, Sabarish R, Zheng T, Pirrami L, Zhang K, Zhang YS, Wan K, Demarchi D, Dokmeci MR, Khademhosseini A, Electrically driven microengineered bioinspired soft robots, Adv. Mater. 30 (2018), 1704189, 10.1002/adma.201704189.

[169]. Ashammakhi N, Ahadian S, Zengjie F, Suthiwanich K, Lorestani F, Orive G, Ostrovidov S, Khademhosseini A, Advances and future perspectives in 4D bioprinting, Biotechnol. J. 13 (2018), 1800148, 10.1002/biot.201800148.

[170]. Gao B, Yang Q, Zhao X, Jin G, Ma Y, Xu F, 4D bioprinting for biomedical applications, Trends Biotechnol. 34 (2016) 746–756, 10.1016/j.tibtech.2016.03.004. [PubMed: 27056447]

[171]. Fetah K, Tebon P, Goudie MJ, Eichenbaum J, Ren L, Barros N, Nasiri R, Ahadian S, Ashammakhi N, Dokmeci MR, Khademhosseini A, The emergence of 3D bioprinting in organ-on-chip systems, Prog. Biomed. Eng. 1 (2019), 12001, 10.1088/2516-1091/ab23df.

[172]. Yang Q, Lian Q,, Xu F, Perspective: fabrication of integrated organon-a-chip via bioprinting, Biomicrofluidics 11 (2017), 10.1063/1.4982945.

[173]. Yi H, Lee H, Cho D, 3D printing of organs-on-chips, Bioengineering 4 (2017), 10.3390/bioengineering4010010.

[174]. Schöneberg J, De Lorenzi F, Theek B, Blaeser A, Rommel D, Kuehne AJC, Kiebling F, Fischer H, Engineering biofunctional in vitro vessel models using a multilayer bioprinting technique, Sci. Rep. 8 (2018) 1–13, 10.1038/S41598-018-28715-0. [PubMed: 29311619]

[175]. Lee VK, Kim DY, Ngo H, Lee Y, Seo L, Yoo S, Vincent PA, Dai G, Biomaterials creating perfused functional vascular channels using 3D bio-printing technology, Biomaterials 35 (2014) 8092–8102, 10.1016/j.biomaterials.2014.05.083. [PubMed: 24965886]

[176]. Kolesky DB, Homan KA, Skylar-scott MA, Lewis JA, Three-dimensional bioprinting of thick vascularized tissues, Proc. Natl. Acad. Sci. U. S. A. 113 (2016) 3179–3184, 10.1073/pnas.1521342113. [PubMed: 26951646]

[177]. Beckwitt CH, Clark AM, Wheeler S, Taylor DL, Stolz DB, Gri L, Wells A, Liver “organ on a chip”, Exp. Cell Res. 363 (2018) 15–25, 10.1016/j.yexcr.2017.12.023. [PubMed: 29291400]

[178]. Bhise NS, Manoharan V, Massa S, Tamayol A, Ghaderi M, A liver-on-a-chip platform with bioprinted hepatic spheroids, Biofabrication. 8 (n.d.) 14101. doi: 10.1088/1758-5090/8/1/014101.

[179]. Homan KA, Kolesky DB, Skylar-scott MA, Herrmann J, Obuobi H, Moisan A, Lewis JA, Bioprinting of 3D convoluted renal proximal tubules on perfusable chips, Sci. Rep. 6 (2016) 1–13, 10.1038/srep34845. [PubMed: 28442746]

[180]. Lind JU, Busbee TA, Valentine AD, Pasqualini FS, Yuan H, Yadid M, Park S, Kotikian A, Nesmith AP, Campbell PH, Vlassak JJ, Lewis JA, Parker KK, Instrumented cardiac microphysiological devices via multimaterial three-dimensional printing, Nat. Mater. 1 (2016) 1–6, 10.1038/NMAT4782.

[181]. Keriquel V, Guillemot F, Arnault I, Guillotin B, Miraux S, Amédée J, Fricain JC, Catros S, In vivo bioprinting for computer- and robotic-assisted medical intervention: preliminary study in mice, Biofabrication 2 (2010), 10.1088/1758-5082/2/1/014101.

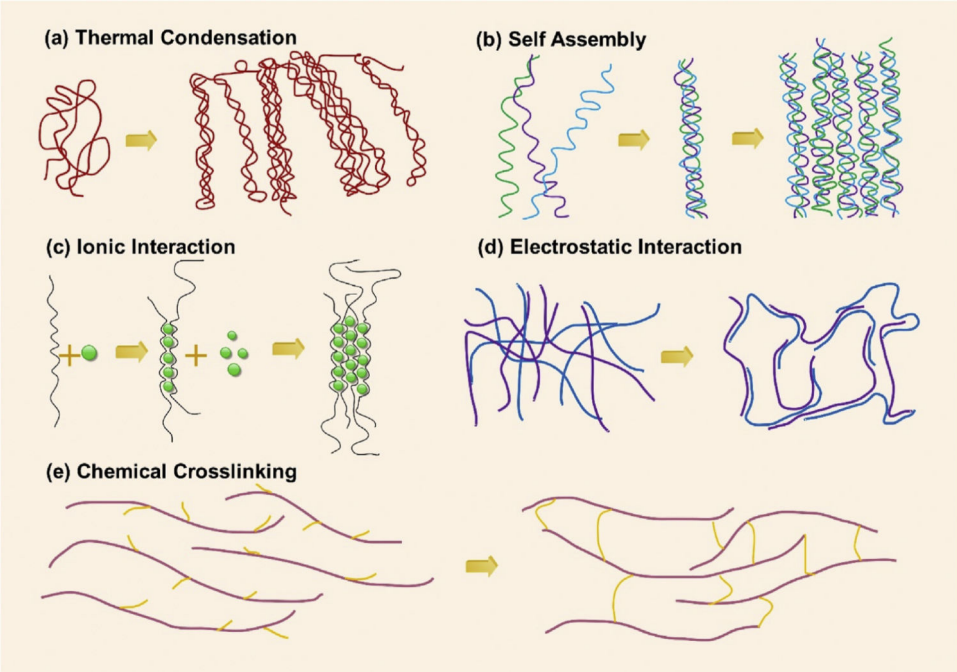

Fig. 1. Crosslinking of hydrogels

(a)-(d) Physical crosslinking: (**a**) Thermal condensation, (**b**) Molecular self-assembly, (**c**) Ionic gelation, (**d**) Electrostatic interaction; and (**e**) Chemical crosslinking.

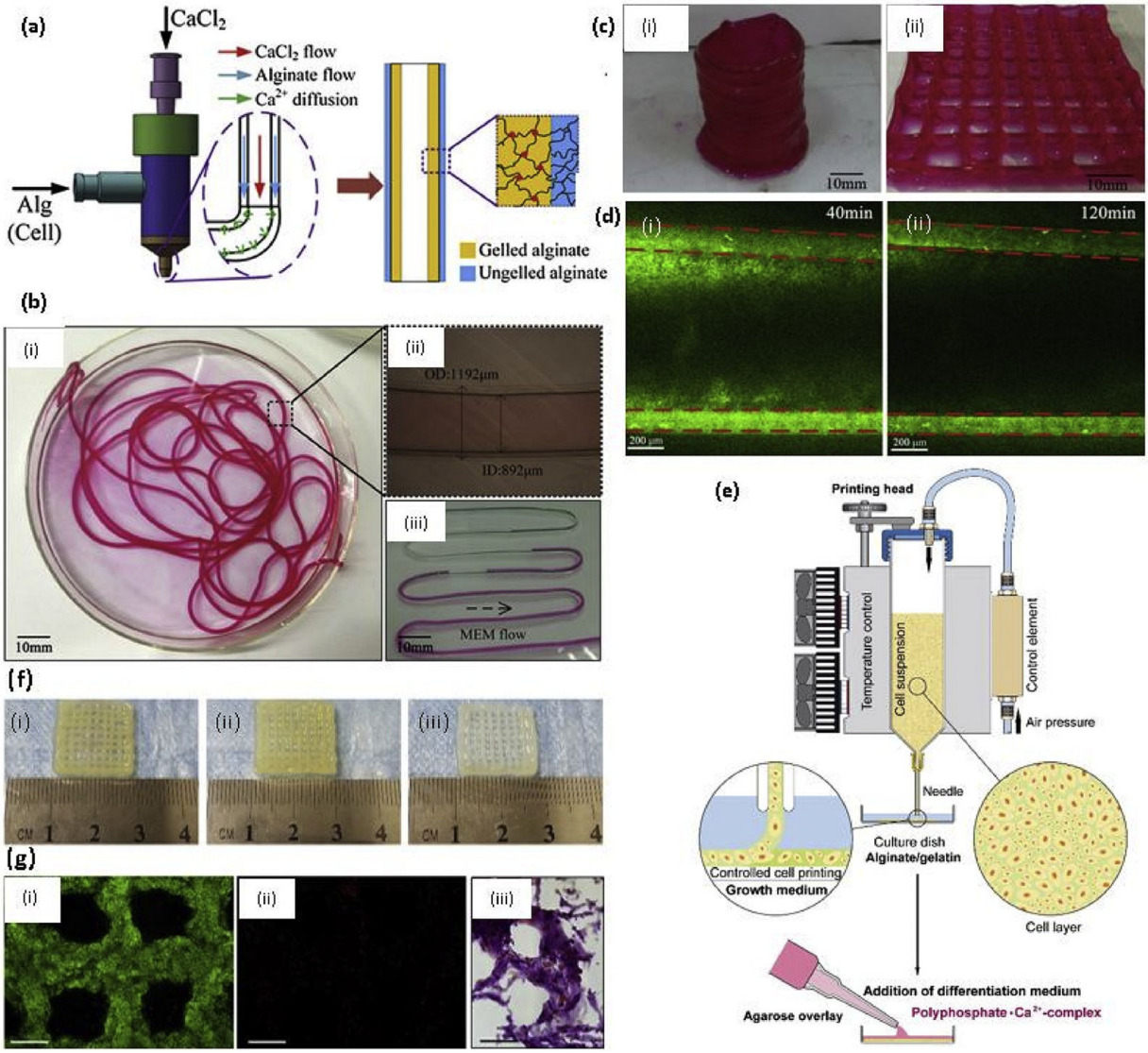

Fig. 2. Natural Polymer based 3D printed hydrogels

(**a**) Coaxial needle used to make hollow tubes, where $CaCl_2$ flows through core nozzle and alginate extrudes through outer nozzle; (**b**) (i) Printed alginate hollow filaments; (ii) The filament under an inverted microscope; (iii) Perfusion of cell culture media (MEM); (**c**) Printed 3D alginate structures with built-in microchannels: (i) Hollow cylinder; (ii) Grid; (**d**) Diffusion mass transfer of EGFP from microchannel into calcium alginate matrix (i) 40min (ii) 120 min [77] with permission from Elsevier, copyright 2015; (**e**) Sketch of the procedure of 3D cell printing of scaffolds subsequently covered with an agarose overlay using the 3D-Bioplotter [86] with permission from Elsevier, copyright 2014; (**f**) 3D bioprinting of chondrocytes encapsulated (i) Sodium alginate (ii) Sodium alginate/agarose (4:1) (iii) Sodium alginate/collagen (4:1) [102] with permission from Elsevier, copyright 2018; and (**g**) 3D bioprinted hyaluronic acid and gelatin matrix with hCMPCs (i) Live-dead assay performed 2h after printing showed the vast majority of hCMPCs to be alive (green) and (ii) Only a few were dead (red), scale bar1000 μm (iii) Hematoxylin and eosin staining 1 day

after printing showed the homogenous distribution of the printed hCMPCs, scale bar 20 μm [111] with permission from Elsevier, copyright 2015. (For interpretation of the references to colour in this figure legend, the reader is referred to the web version of this article.)

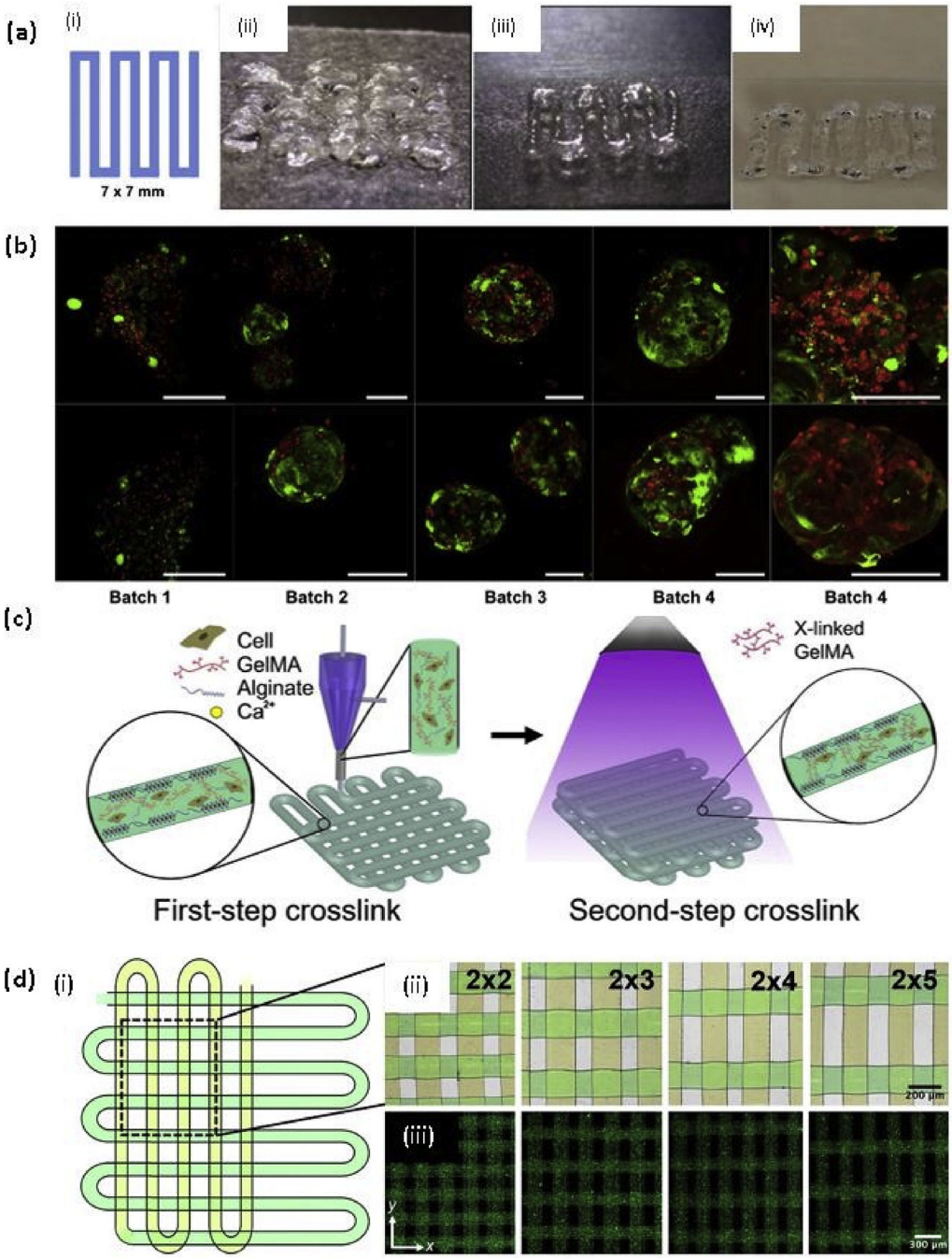

Fig. 3. Gelatin and methacrylated gelatin based bioprinting

(**a**) Testing of bioinks, (i) A 7 × 7 mm pattern used for bioink deposition. (ii) An initial formulation of a PEGDA and 4-arm PEG alkyne containing bioink. (iii) Improved extrusion and end structure smoothness after addition of unmodified HA and gelatin to improve shear thinning and material smoothing. (iv) Extruded hydrogel bioink formulation using 8% PEGDA and 8% 8-arm PEG alkyne crosslinkers; (**b**) Demonstration of bioprinting parameter optimization and associated viability of liver spheroids bioprinted in the liver-specific hydrogel bioink resulted in high cell viability as depicted using LIVE/DEAD

viability assay (batch 1–4). In contrast, gelatin-based gels that were printed in parallel under optimal environmental conditions yielded extremely poor viability (batch 5). Green - calcein AM-stained viable cells; Red - ethidium homodimer-stained dead cells. Scale bars - 200 μm [122] with permission from Elsevier, copyright 2015; (**c**) Schematic diagrams showing the two-step crosslinking process, where the alginate component is first physically crosslinked by the CaCl2 followed by chemical crosslinking of the GelMA component using UV illumination; and (**d**) (i)Top view single-layer schematic of the design of the bioprinted microfibrous scaffold and corresponding (ii) Brightfield (pseudocolored to match the schematic) and (iii) Fluorescence micrographs showing the bioprinted scaffolds with different aspect ratios of unit grids [131] with permission from Elsevier, copyright 2016. (For interpretation of the references to colour in this figure legend, the reader is referred to the web version of this article.)

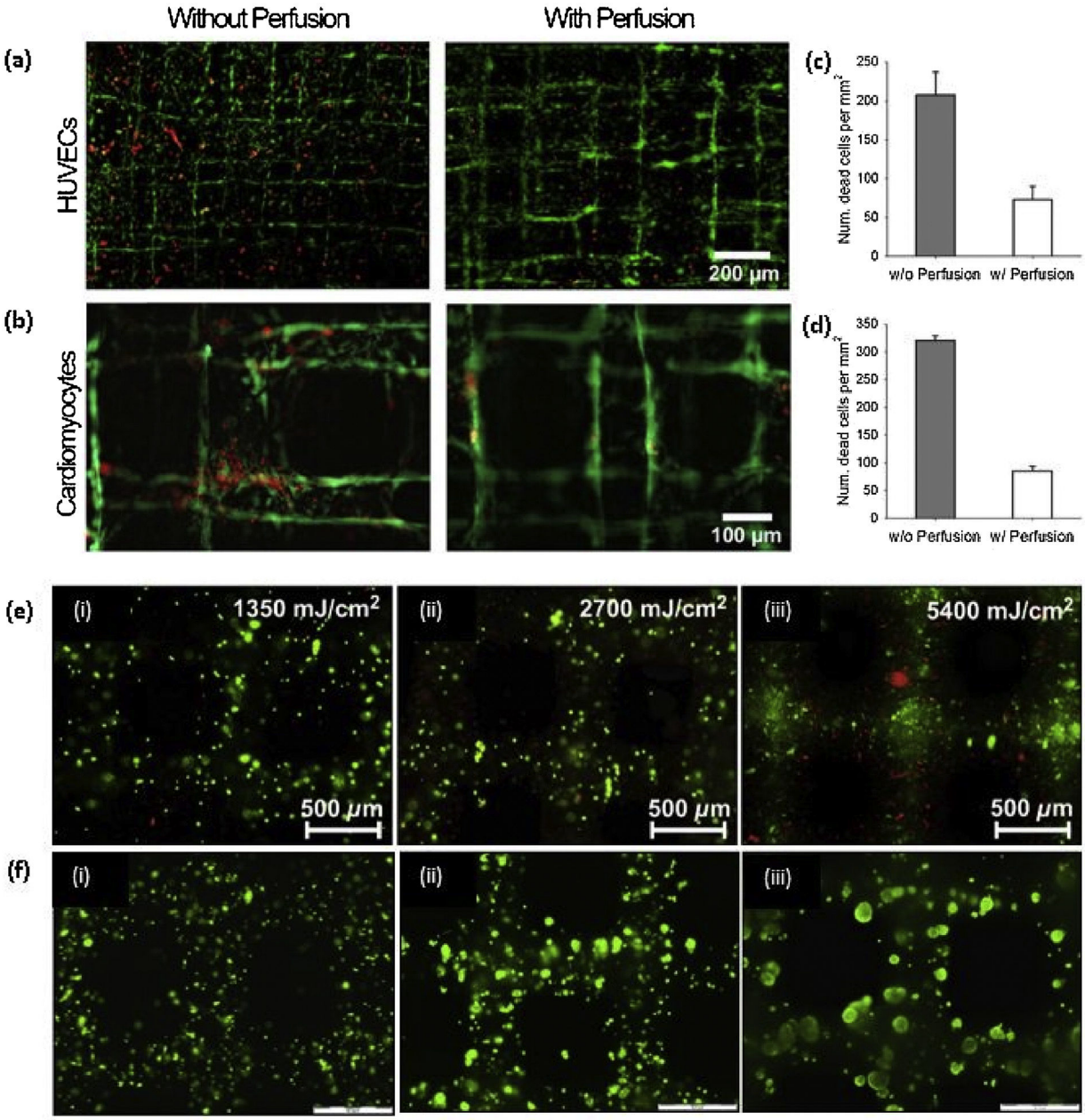

Fig. 4. GelMA based bioprinting

(**a, b**) Live/dead micrographs and quantified cell morbidity of bioprinted endothelialized scaffolds without and with perfusion in the bioreactors; (**c, d**) Live/dead micrographs and quantified cell morbidity of bioprinted cardiac organoids without and with perfusion in the bioreactors [131] with permission from Elsevier, copyright 2016; (**e**) HepG2-gelatin constructs were cured using 12959 and an irradiation dose of (i) 1350, (ii) 2700, and (iii) 5400mJ/cm^2. After 24h, cell survival was evaluated using a LIVE/DEAD assay. Scale bar indicates 500 μm; (f) HepG2-gelatin constructs, cured using the VA-086 photo initiator with irradiation dose of 1800mJ/cm^2, Cell viability within the scaffold was evaluated at (i) Day 1, (ii) Day 7, and (iii) Day 14 using a live/dead stain; (scale bar 500 μm) [132] with permission from Elsevier, copyright 2014.

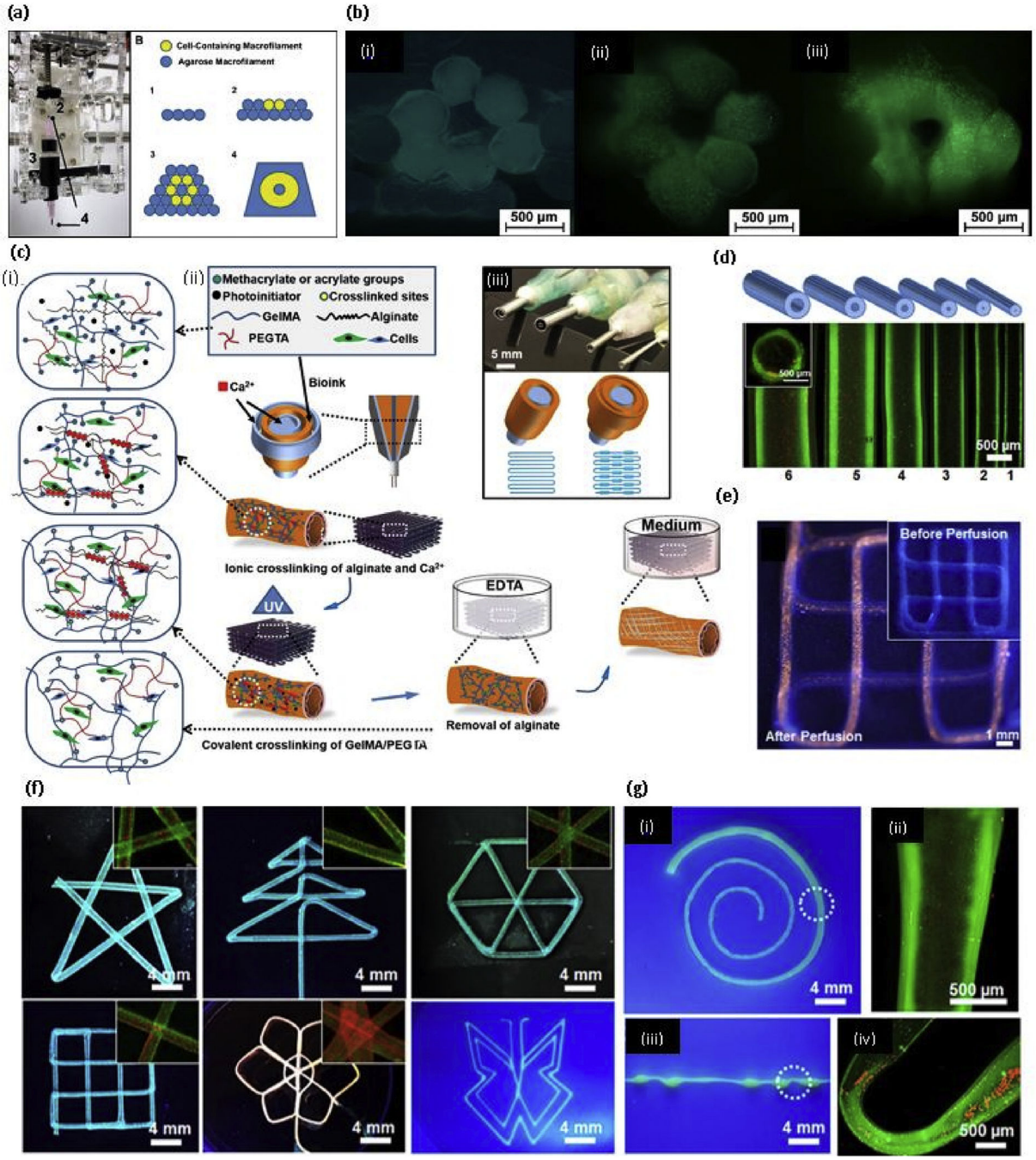

Fig. 5. PEG based bioprinting

(**a**) The custom microcapillary tube adaptor and printing protocol for building a cellularized tubular structure, consisting of depositing hydrogel macrofilaments in a stacked manner; (**b**) (i) Immediately after printing (ii) At 14 days, and (iii) At 28 days of culture using LIVE/DEAD staining to highlight viable and dead cells [141] with permission form Elsevier, copyright 2010; (**c**) (i) Schematic diagram showing two step crosslinking processes of the bioink, (ii) Schematics showing the procedure of bioprinting perfusable hollow tubes with the bioink (iii) The designed multilayered coaxial nozzles; (**d**) Fluorescence micrographs

showing the bioprinted perfusable tubes displaying different outer diameters; (**e**) Fluorescence photographs before (inset) and after injection with red fluorescent microbeads into the lumen of the single, continuous bioprinted tube (**f**) Fluorescence photographs showing bioprinted perfusable tubes with various shapes; and (**g**) Photographs showing single tubes bioprinted with a gradually increasing size (i) and periodically varying sizes (iii) the high-magnification fluorescence micrographs in (ii and iv) clearly show the varying diameters at selected locations indicated in (i and iii), respectively [142] with permission from Elsevier, copyright 2016. (For interpretation of the references to colour in this figure legend, the reader is referred to the web version of this article.)

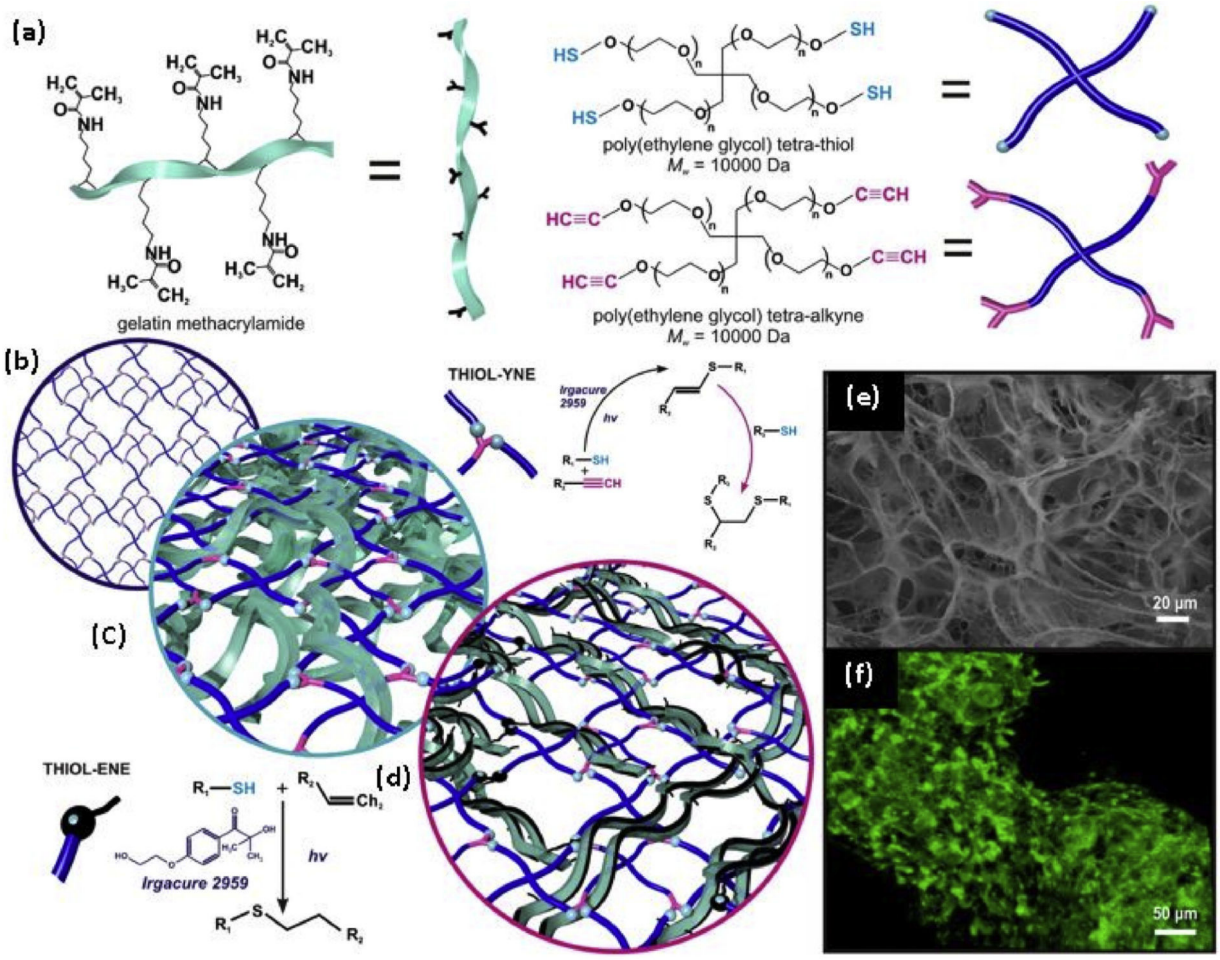

Fig. 6. Fabrication of bio/synthetic interpenetrating network

(BioSIN) of (**a**) Gelatin methacrylamide and poly(ethylene glycol) *via* concurrent photoinitiation of thiol-ene and thiolyne coupling. The click-functionalized macromer precursors undergo multi-mode crosslinking to form an interlocking 3D hydrogel; (**b**) The well-defined network architecture of TYC-formed PEG hydrogels were intertwined with either; (**c**) Physically-incorporated gelatin (BioSINP) or; (**d**) Covalently crosslinked gelatin methacrylamide (BioSINx) in which the gelatin methacrylamide reacts with both itself and the PEG network.; (**e**) The architectural heterogeneity emulated native extracellular matrix; (**f**) Superior physiochemical properties were able to support the continued proliferation of encapsulated cells, where cytoskeletal F-actin fiber staining illustrates the density and interaction of encapsulated cells [150] with permission from Elsevier, copyright 2014.

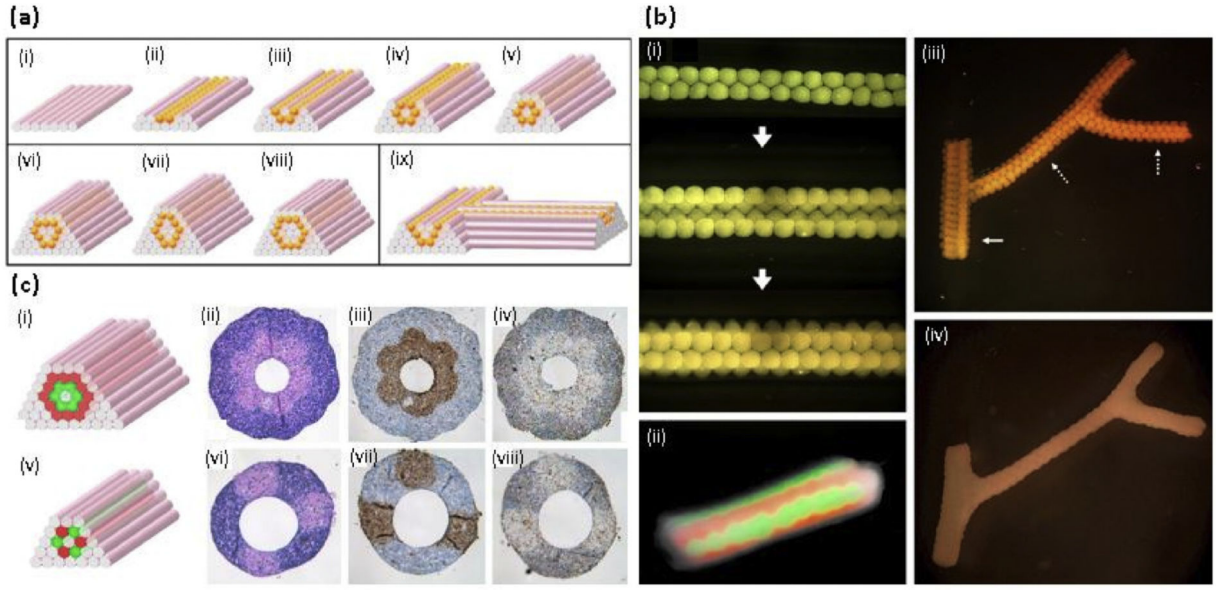

Fig. 7. Scaffold-free bioprinting

(**a**) Design template for tubular structures. (i-v) Deposition scheme for the smallest diameter tube that can be built of agarose rods (pink) and multicellular spheroids (orange) of the same diameter. (vi-viii) More complex tubular structures. (ix) Scheme for a branching structure. (**b**) Fusion patterns of multicellular spheroids assembled into tubular structures. (i) HSF spheroids assembled according to the template. (ii) Fusion pattern after 7 days of a tube assembled from fluorescently labeled red and green sequences of CHO spheroids. (iii) Branched structure built of 300 mm HSF spheroids with branches of 1.2 mm (solid arrow) and 0.9mm (broken arrows). (iv) The fused branched construct after 6 days of deposition. (**c**) Building a double-layered vascular wall; i,v. HUVSMC and HSF multicellular cylinders were assembled according to specific patterns (HUVSMC: green; HSF: red). Panels ii-iv and vi-viii show the results of histological examination of the respective structures in i and v after 3 days of fusion: H&E (ii,vi), smooth muscle a-actin (brown; iii,viii) and Caspase-3 (brown; iv,viii) stainings are shown. Note that the more complex construct in the upper row requires more time to fuse [23] with permission from Elsevier, copyright 2009. (For interpretation of the references to colour in this figure legend, the reader is referred to the web version of this article.)

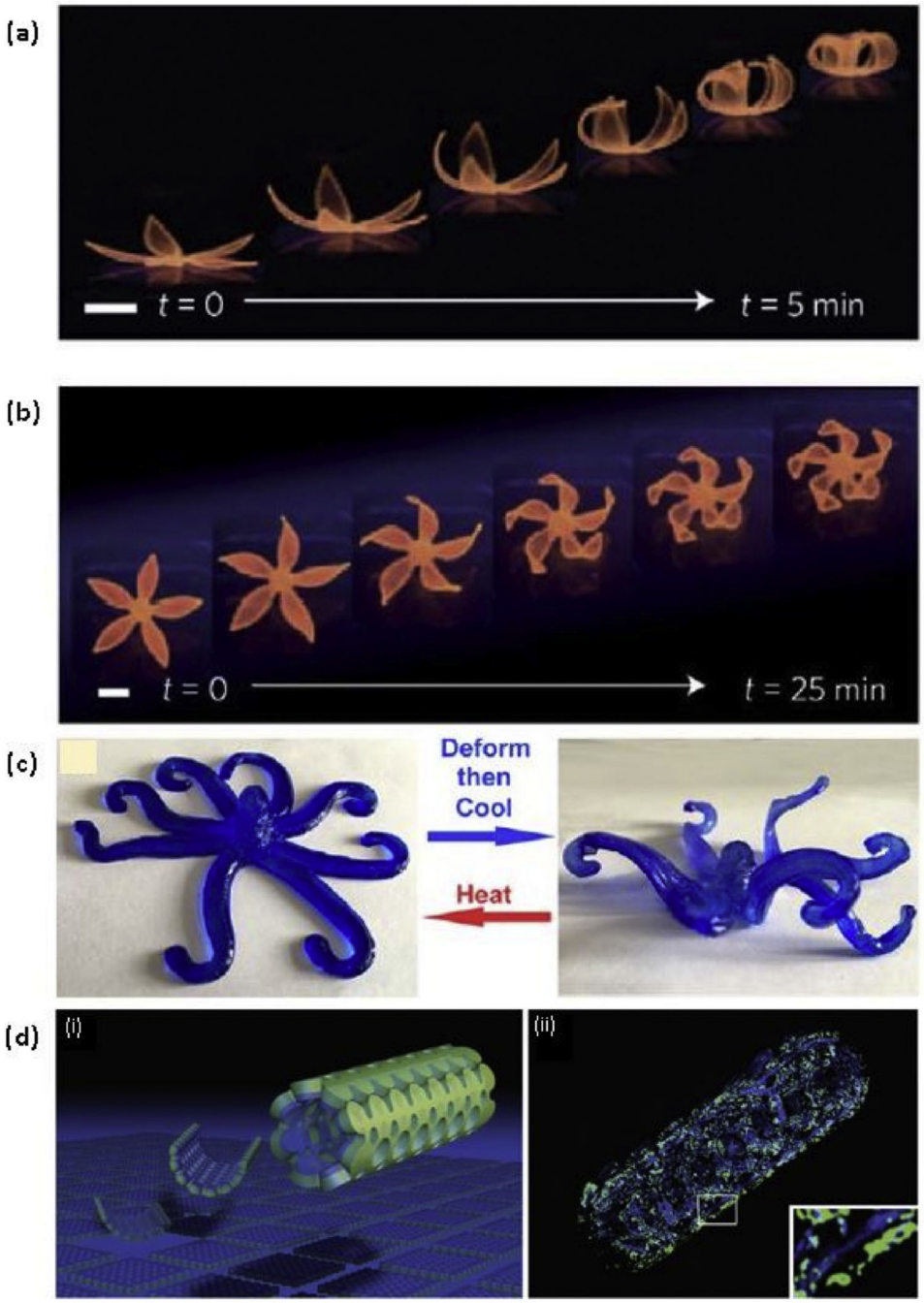

Fig. 8. 4D bioprinting

(**a**) Complex flower morphologies generated by biomimetic 4D printing; Simple flowers composed of 90°/0° (**b**) and −45°/+45° bilayers oriented with respect to the long axis of each petal, with time-lapse sequences of the flowers during the swelling process [157] with permission from Springer Nature, copyright 2016; (**c**) The softening and hardening cycles of an octopus like gel [165] with permission from ACS, copyright 2018; (**d**) Multi-culture of cells in distinct layers of a self-folded hydrogel. (i) Conceptual schematic illustrating the self-folding of an initially planar PEG bilayer that contains different populations of cells in

the inner (blue) and outer (green) hydrogel layers. (ii) A deconvoluted fluorescent micrograph of a self-folded bilayer containing Hoechst-stained fibroblasts (blue) in the inner hydrogel layer and calcein AM-stained fibroblasts (green) in the outer hydrogel layer [166] with permission from John Willy and Sons, copyright 2014.(For interpretation of the references to colour in this figure legend, the reader is referred to the web version of this article.)

Table 1

Comparison of bioprinter types.

	Bioprinter type			Stereolithography	Refs.
	Drop on demand (inkjet)	Microextrusion	Laser-assisted		
Material viscosities	3.5–12 mPa/s	30 mPa/s to above 6×10^7 mPa/s	1–300 mPa/s	No limitation	[1,9,14,15,16]
Print speed	Fast	Slow	Medium	Fast	[1,9,12,17]
Resolution or droplet size	High	Moderate	High	High	[1,9,18]
Printer cost	Low	Medium	High	Low	[1,9,17,19]
Cell viability	80–95%	40–90%	<85%	>85%	[1,17,20,21]
Cell densities	Low < 10^6 cells/ml	High (cell spheroids)	Medium, 10^8 cells/ml	Medium	[9,17]
Preparation time	Low	Low to medium	High	Low	[22,23,18]
Materials used in bioprinting	Alginate, collagen	Alginate, GelMA, PEGDMA, PEGDA	Collagen, Martigel	Hyaluronic acid Alginate, PEG based acrylates	[1,18]

Appl Mater Today. Author manuscript; available in PMC 2020 August 08.

Table 2

The advantages and disadvantages of each hydrogel type with their respective application in the biomedical field.

Hydrogel type	Advantages	Disadvantages	Applications	References
Alginate	Viscosity can be easily manipulated by changing the concentration Comparatively short cross-linking time $CaCl_2$ does not significantly reduce the cell viability Compatible with a lot of cell types	Mechanically unstable for prolonged culture Low degradation rates Does not enhance the cell proliferation	Vascular tissue Cartilage tissue Bone tissue	[81] [83,89] [85,90]
Collagen	Natural ECM material Act as a good cell carrier Can easily mix with other hydrogels, such as alginate, GelMA, PEG-based derivatives	Low mechanical stability and cannot be used alone Prolonged crosslinking time	Cartilage tissue Skin tissue	[94,96] [99–101]
Chitosan	Natural material Shows relatively good mechanical stability Can easily mix with other hydrogel materials	Acidity reduces the cell viability Neutralization of the solution is required. Can not be used alone	Bone tissue	[107]
Hyaluronic acid	A major component of the ECM Act as a good cell carrier Facilitates cell proliferation Can easily modify and mix into different hydrogel systems to increase mechanical stability and cell viability	Low mechanical stability and cannot be used alone	Cardiovascular tissue Cartilage tissue	[111] [113]
Gelatin	Consists of natural ECM components Have thermo-responsive property Good cell viability Can use as cell carrier or fugitive bio-ink	Low mechanical stability Not stable at physiological temperature	Vascular tissue Liver tissue	[118,121] [122]
Gelatin methacrylate	Derived from modification of gelatin, and consists of natural ECM component Light polymerizable into the stable hydrogel Short cross-linking time Compatible with many cell types	Low mechanical stability Cell viability depends on the photocrosslinking time, the intensity of the light and photoinitiator	Vascular tissue Myocardium-on-chip Liver tissue Cartilage tissue	[129] [131] [132,134] [137]
PEG-based derivatives	Properties of the PEG-based derivatives can be easily manipulated using chemical modification techniques Good mechanical stability can be achieved Shows relatively good mechanical stability Mostly light polymerizable material within a short time	Synthetic material Does not provide biological cues for cell proliferation Cell viability depends on the photocrosslinking time, the intensity of the light, and photoinitiator	Vascular tissue Bone tissue Cartilage tissue	[142,143] [145,146,147] [145,147]